

# Newsletter

No. 165 | Autumn 2020

Using the EFI for water vapour flux

---

Weather regimes in predictions for Europe

---

CAMS contributes to study of COVID-19 links

---

Progress towards a European Weather Cloud

---

© Copyright 2020

European Centre for Medium-Range Weather Forecasts, Shinfield Park, Reading, RG2 9AX, UK

The content of this Newsletter is available for use under a Creative Commons Attribution-Non-Commercial-No-Derivatives-4.0-  
Unported Licence. See the terms at <https://creativecommons.org/licenses/by-nc-nd/4.0/>.

The information within this publication is given in good faith and considered to be true, but ECMWF accepts no liability for error or omission or for loss or damage arising from its use.

---

### **Publication policy**

The ECMWF Newsletter is published quarterly. Its purpose is to make users of ECMWF products, collaborators with ECMWF and the wider meteorological community aware of new developments at ECMWF and the use that can be made of ECMWF products. Most articles are prepared by staff at ECMWF, but articles are also welcome from people working elsewhere, especially those from Member States and Co-operating States.

The ECMWF Newsletter is not peer-reviewed.

Any queries about the content or distribution of the ECMWF Newsletter should be sent to [Georg.Lentze@ecmwf.int](mailto:Georg.Lentze@ecmwf.int)

Guidance about submitting an article and the option to subscribe to email alerts for new Newsletters are available at [www.ecmwf.int/en/about/media-centre/media-resources](http://www.ecmwf.int/en/about/media-centre/media-resources)

## Adjustments

As I write this editorial, the UK and much of Europe is going into a further lockdown because of COVID-19. The weather and climate community has adjusted to the situation quickly and efficiently. At ECMWF, all our workshops, training courses and seminars are being held virtually. This decision is based on the need to continue to collaborate closely with our partners. For example, more than 300 researchers from across the world joined the ECMWF Annual Seminar 2020. Held in September, it presented the state of the art in computational methods for solving the equations that govern atmospheric, wave, ocean and sea-ice dynamics. Other recent online events include the first ECMWF-ESA (European Space Agency) workshop on machine learning for Earth system observation and prediction and the ECMWF-EUMETSAT meeting on the treatment of random and systematic errors in satellite data assimilation for numerical weather prediction.

Another strand of work that has continued apace is building our new data centre in Bologna, Italy. The renovation work of the existing factory building is now nearly complete, and the new supercomputer can soon be moved in. Watch this editorial for further updates on progress.

What has been keeping us busy in Reading, UK, is documented in this Newsletter. An article of particular interest is the one about weather regimes in extended predictions for Europe. It discusses a few different regime definitions for the Euro-Atlantic region and shows examples of useful visualisations. An article on the Extreme Forecast Index for water vapour flux examines the usefulness of this new product for mid-latitude storms and provides guidance on its use. The World Meteorological Organization's Year of Polar Prediction (YOPP) has found a warm bias in

temperature predictions, including in ECMWF forecasts. And we found that the prediction of Hurricane Laura, which hit Louisiana in the United States as a category 4 hurricane, could have been better if we had used a finer ensemble forecast grid spacing.



Other articles examine progress towards making ECMWF forecasts available on new cloud technology and the use of the European Commission's Copernicus Atmosphere Monitoring Service (CAMS), run by ECMWF, to help study air pollution links to COVID-19. The latter article takes us back to the effects of the pandemic on Europe and the globe. It shows that there is an upside: a substantial decrease of certain air pollutants in many areas as lockdown effects are introduced.

The effects of the pandemic for the weather and climate community are thus felt in multiple ways. They include not just a break on person-to-person exchanges and a reduction in the availability of some types of Earth system observations, but also a reduction in air pollution because of local lockdowns. We are not only adapting to the situation through our work practices and use of data but are also examining the consequences of the pandemic together with the scientific community.

**Florence Rabier**  
Director-General

## Contents

### Editorial

Adjustments ..... 1

### News

Hurricane Laura and its threat to the United States ..... 2  
Using ECMWF data for humanitarian support ..... 4  
ECMWF analyses detect vortices generated by 2019/20 Australian wildfires ..... 5  
GloFAS helps Bangladesh flood forecasters to predict monsoon flood ..... 6  
The YOPP site inter-comparison project ..... 7  
Using the EFI for water vapour flux at the UK Met Office Flood Forecasting Centre ..... 9  
Understanding how forecast users make decisions ..... 10  
The life of GLAMEPS ..... 12

New observations since July 2020 ..... 13

### Meteorology

How to make use of weather regimes in extended-range predictions for Europe ..... 14  
CAMS contribution to the study of air pollution links to COVID-19 ..... 20

### Computing

Progress towards a European Weather Cloud ..... 24

### General

Contact information ..... 27  
ECMWF publications ..... 28  
ECMWF Calendar 2020/21 ..... 28

# Hurricane Laura and its threat to the United States

Linus Magnusson, Simon Lang (both ECMWF), Sharan Majumdar (ECMWF; University of Miami, USA)

On 27 August 2020, Hurricane Laura made landfall in southwestern Louisiana as a category 4 hurricane, making it one of the most intense cyclones to make U.S. landfall based on maximum sustained wind speed. The effects of the hurricane were a damaging storm surge, extreme winds, and coastal and inland flooding. However, the impacts could have been much larger if the cyclone had hit the metropolitan area of Houston, Texas, with approximately seven million residents and large oil and petrochemical industries. Prior to its intensification into a hurricane, Tropical Storm Laura caused substantial damage in the Caribbean, especially Haiti, the Dominican Republic, and Cuba, including several dozen fatalities.

The tropical cyclone originated from an African Easterly Wave that propagated from western Africa into the Atlantic around 15 August. At this stage ECMWF's ensemble forecast predicted the risk for the genesis of the cyclone, but with high uncertainties about the future path and duration of the system. For example, the ensemble from 17 August included a few members

with a cyclone entering the Gulf of Mexico, but also members hitting Florida and curving north over the Atlantic, and with many members where the cyclone quickly dissipated.

## Predictions in the Gulf of Mexico

The cyclone was recognised as a tropical storm on 21 August while being east of the Leeward islands. The cyclone passed over land on Hispaniola and Cuba and entered the Gulf of Mexico on 25 August as a weak cyclone. At this point the ensemble predicted a landfall on the north-western coast of the Gulf on 27 August, but with large uncertainties. This is a region with sharp gradients in the population, and a relatively small difference in the landfall position would result in huge differences in the human impact. In the forecast from 00 UTC 25 August, the city of Houston, Texas, was in the middle of the ensemble plume. This was a critical time for local officials to decide whether or not to issue a mass evacuation order for the city. This remains a sensitive issue given the chaotic evacuation ahead of Hurricane Rita in 2005, which resulted in over 100 fatalities. On the morning

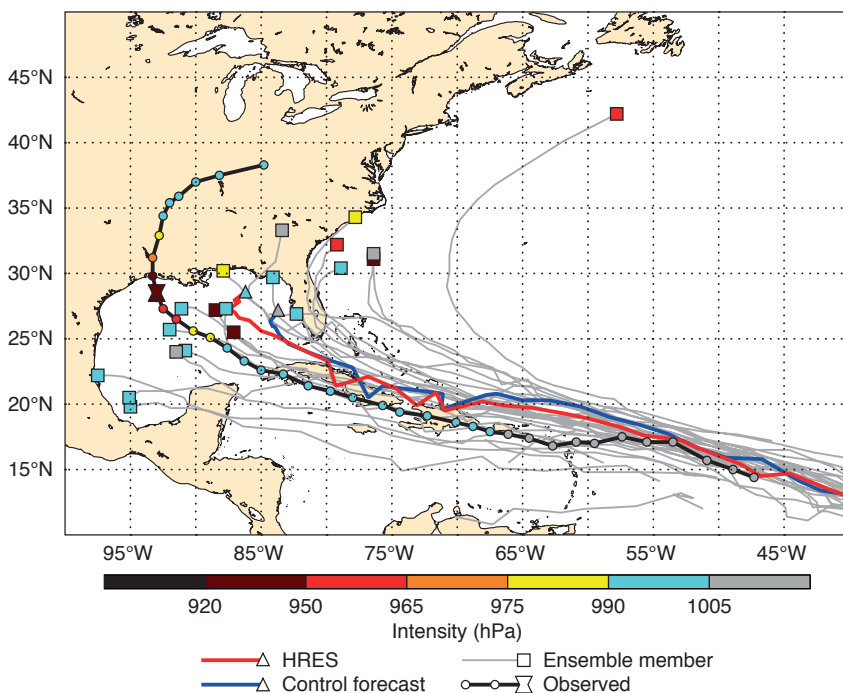
of 25 August 2020, the United States National Hurricane Center reviewed all the latest operational numerical model and ensemble forecasts, and they decided to nudge the forecast landfall location slightly nearer to Houston than their previous forecast, but not directly at Houston. As a result, no mandatory evacuation order was issued for greater Houston, with only the local barrier islands being evacuated at that time. On 26 August, the ensemble plume shifted further to the east and eventually the hurricane made landfall on the coast of Louisiana, with Houston receiving only minor impacts.

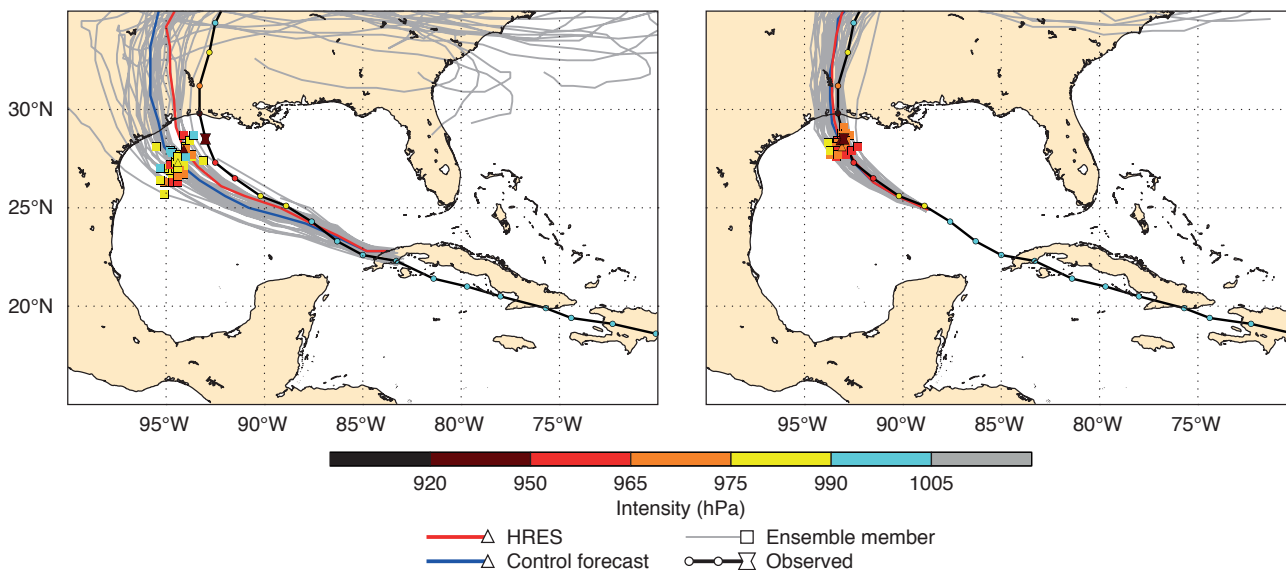
It was noted by many users that on 24–25 August the ECMWF high-resolution (HRES) forecast was located on the eastern edge of the ensemble plume, which posed the question if the lower resolution of the ensemble degraded the result. To test this hypothesis, subsequent experimental ensemble forecasts with the same resolution as HRES were run for the forecasts from 23 August 00 UTC to 25 August 12 UTC. These experimental ensembles were indeed more centred around the HRES forecast and resulted in substantially improved forecasts for most dates, with a systematic shift of the plumes to the east. However, still most members of the experimental ensemble from 25 August (both 00 and 12 UTC) had landfall to the west of the eventually observed landfall point. The exception regarding improvement was the forecast from 23 August 12 UTC, where the eastward shift led to larger errors in the sense of the ensemble mean.

## Intensity forecast

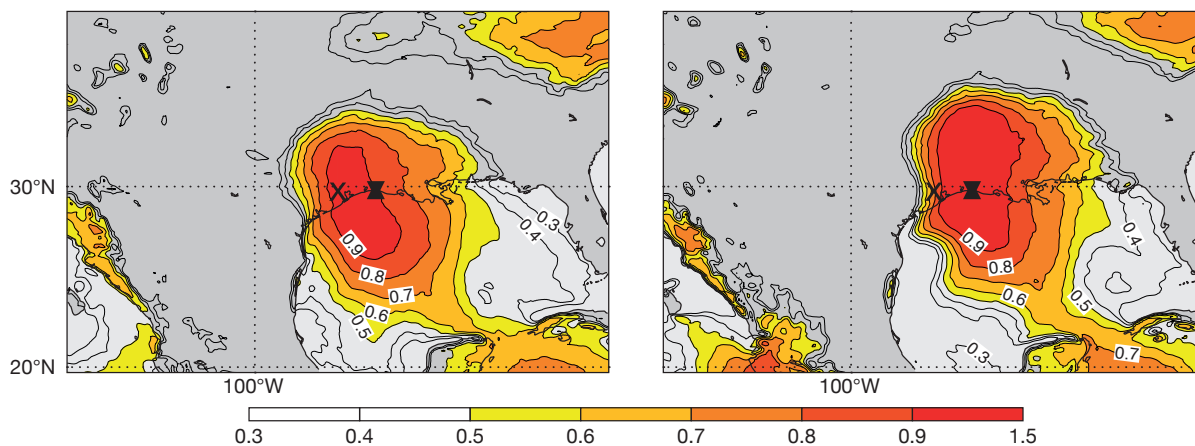
The experimental ensemble also captured the intensity forecast far better than the current operational ensemble due to the higher model resolution. The ensemble gave a good indication of the rapid intensification of the cyclone over the Gulf of Mexico on

**Early prediction.** Track forecasts from 17 August 00 UTC, with position markers valid for 27 August 00 UTC.

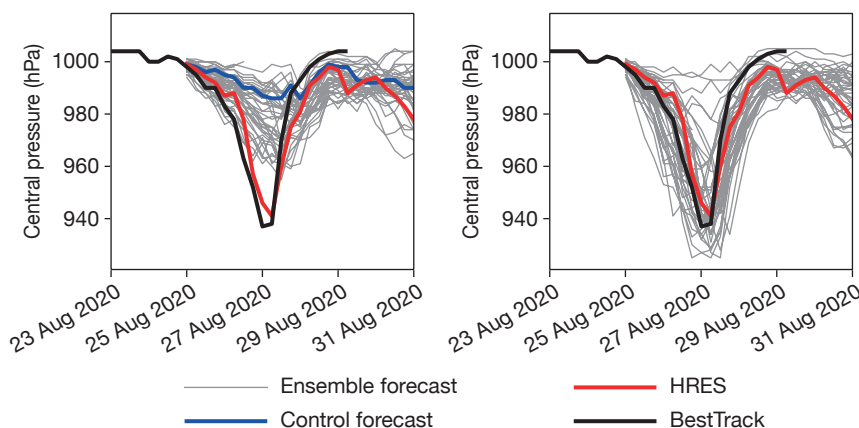




**Landfall predictions.** Track forecasts from 25 August 00 UTC (left) and 26 August (right) with position markers valid for 27 August 00 UTC.



**Extreme Forecast Index for wind gusts.** Extreme Forecast Index (EFI) for 10-metre wind gusts valid on 27 August, from 25 August 00 UTC (left) and 26 August (right). The cross symbol marks Houston, Texas. The landfall location is shown as the hourglass. The Shift of Tails product, which focuses on the higher end of the extreme, shows a similar shift of the risk of 10-metre wind gusts to the right.



**Current and experimental intensity forecasts.**

Forecasts of the central pressure comprising the operational ensemble forecast, control forecast, high-resolution forecast (HRES) and preliminary BestTrack data (left) and HRES and preliminary BestTrack data with the experimental ensemble with the same resolution as HRES (right).

26 August. The maximum wind speed in the cyclone was reasonably captured, a result of the model upgrade in Integrated Forecasting System Cycle 47r1, reported in the Spring 2020 issue of the ECMWF Newsletter.

**Open dataset and summary**

The challenging forecasts for this case pose several research questions. To facilitate further research on the details of the ensemble forecasts, ECMWF has

archived the full vertical resolution for the operational ensemble forecasts for TC Laura. This dataset would make it possible to do detailed studies of the tropical cyclone structure in the ensemble members, and also to downscale the system with limited-area models for detailed impact studies. The plan is to make this dataset available for the research community to facilitate further research.

# Using ECMWF data for humanitarian support

Emma Pidduck, Umberto Modigliani

ECMWF’s Council has approved the provision of ECMWF real-time products to international organisations including UN and European Commission agencies for operational purposes to further support World Meteorological Organization (WMO) programmes and activities. The move comes in addition to providing the WMO Additional dataset to the national meteorological and hydrological services (NMHS) of WMO countries, in June and December 2017 (<https://www.ecmwf.int/en/forecasts/datasets/wmo-additional>).

Since the approval, UN and European Commission agencies such as the United Nations World Food Programme, the European Maritime Safety Agency (EMSA), the European Commission Joint Research Centre (JRC) and the European Civil Protection and Humanitarian Aid Operations (DG-ECHO) have been using ECMWF data for their operational activities, and more recently UNICEF has requested access to ECMWF’s ecCharts platform for operational support.

## Benefits

One example of the benefits of providing data to the various agencies is the Automated Disaster Analysis

and Mapping (ADAM) alert system, which is compiled and distributed by the United Nations World Food Programme (WFP). The emergency response dashboard is issued by the WFP to the humanitarian community to support regions that might be impacted by environmental hazards, such as tropical storms, flash flooding, and earthquakes.

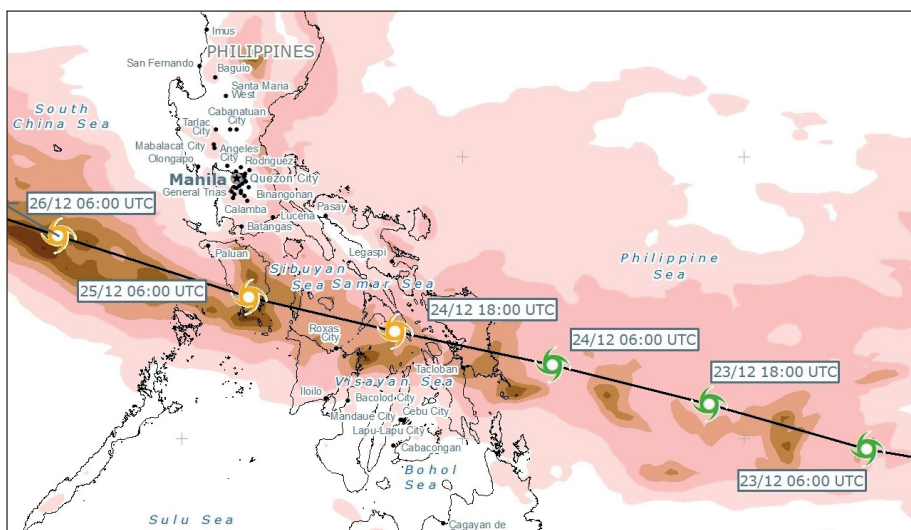
The application was started in 2015 as an earthquake alert response. In 2017, it was expanded to monitor the impact of tropical storms by using data from several authoritative sources such as, among others, the Joint Research Centre, the US Geological Survey, the World Bank, the US National Oceanic and Atmospheric Administration (NOAA) and WFP databases. Since June 2018, the WFP has used ECMWF deterministic total precipitation data in combination with tropical cyclone data to show the expected rainfall for the next five days for key cities that may be affected by a tropical storm (see figure). ADAM enables WFP and other humanitarian agencies to make well-informed decisions and to carry out more informed preparation for emergencies, including knowing exactly where to position food or identifying different access routes to critical areas.

“Timeliness of response is one of the

most critical factors to save lives in emergencies,” says Project Coordinator Andrea Amparore of the WFP Emergency Division. “Just seconds after an earthquake occurs, or days before a tropical storm makes landfall, ADAM provides the right information, to the right people, at the right time.”

Since 2017, the WFP has issued dozens of dashboards to about 5,000 registered users, covering all major tropical cyclones worldwide, including Idai (Mozambique, March 2019), Michael (Caribbean, October 2018), and Maria (Caribbean, September 2017). In 2020, the WFP received the Nobel Peace Prize for its efforts to combat hunger and improve conditions for peace.

The ADAM dashboard is distributed to registered users of humanitarian organisations to receive the dashboards directly to their inbox in real time. Registration is free (<https://geonode.wfp.org/adam.html>) for users working for humanitarian organisations, governments, and universities. Moreover, in order to allow the general public to reach the service, ADAM dashboards are also published on Twitter (@WFP\_ADAM) in response to emergency events.



**Example of a tropical cyclone forecast.** An example ADAM dashboard showing the predicted 5-day accumulated precipitation for each city impacted during tropical cyclone Phanfone, which passed over the Philippines in December 2019.

Predicted wind speed  
 < 110 km/h  
 110 – 185 km/h  
 185 – 240 km/h  
 > 240 km/h

Five-day accumulated precipitation (mm)  
 < 20    50 – 100    150 – 200    250 – 350  
 20 – 50    100 – 150    200 – 250    > 350

# ECMWF analyses detect vortices generated by 2019/20 Australian wildfires

Sergey Khaykin, Bernard Legras, Silvia Bucci, Pasquale Sellitto (all IPSL, Paris, France), Lars Isaksen (ECMWF)

A research study by scientists from France and ECMWF has revealed the ability of the operational ECMWF Integrated Forecasting System (IFS) to accurately analyse long-lived smoke-charged vortices in the stratosphere.

## The ECMWF analysis

The Australian ‘Black Summer’ was marked by exceptionally strong pyro-cumulonimbus (PyroCb) activity in the south-east of the continent, with 5.8 million hectares of forest burnt. The strongest PyroCb outbreak occurred on New Year’s Eve. It lofted a colossal cloud of smoke-ice mixture to 15 km altitude. Already two weeks later, it became clear from satellite observations that the magnitude of stratospheric perturbation from this single PyroCb event had tripled that of the record-breaking 2017 Canadian wildfires. The biggest surprise came when we realized that the ECMWF operational IFS analyses were revealing an organised anticyclonic vortex that encompassed the rising smoke bubble. This vortex, created and maintained by the localized radiative heating of the absorbing smoke cloud, kept the bubble confined by strong winds during its

entire life. The left panel of the figure shows a vertical cross section of the smoke cloud observed by the CALIOP space-based lidar instrument on 31 January 2020. The large smoke bubble had a vertical extent of 5 km and horizontal extent of 1,000 km. The other panels of the figure show that the IFS was able to analyse the anticyclonic vortex (large potential vorticity) and the extensive warming at the bottom/cooling at the top of the vortex. It lasted for about three months, during which it travelled 66,000 km and rose from 16 to 35 km. The whirling bubble contained not only the smoke particles but also several megatons of water and carbonaceous gases. Ozone concentrations were found to be very low inside the bubble, thereby creating a synoptic-scale ozone hole.

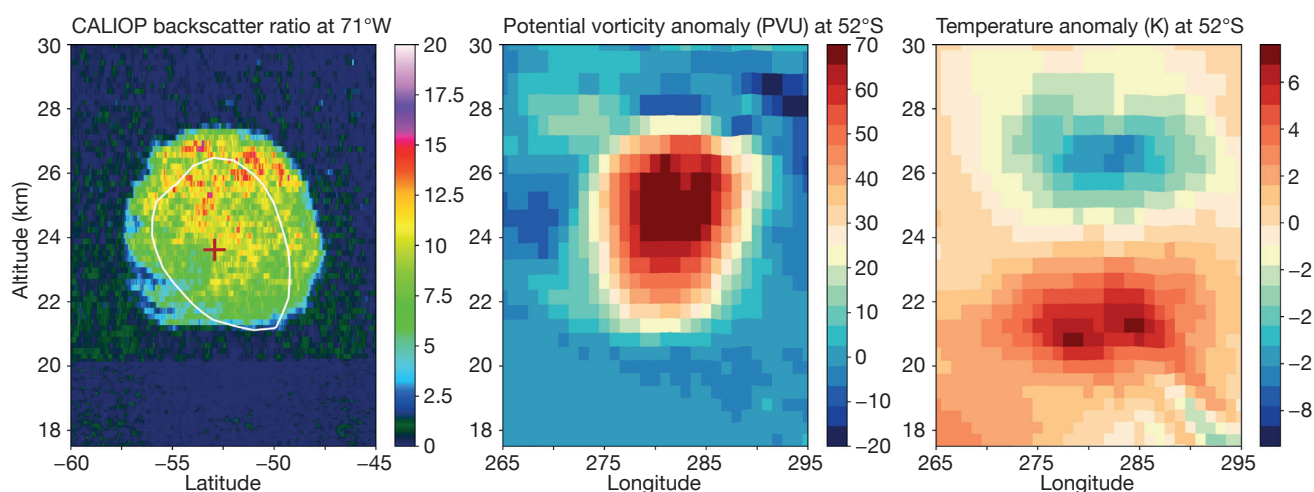
## Understanding smoke clouds

The operational IFS only uses aerosol climatology, so the smoke cloud was not analysed directly. It is a remarkable achievement that the ECMWF analysis still managed to detect the smoke bubble. This was due to the thermal signature of the vortex, a vertical dipole of  $\pm 5$  K. The thermal signature

was primarily detected by hyperspectral sounders (e.g. IASI, AIRS and CriS) and GPS radio occultation data (primarily from Metop), which are assimilated by the IFS. Hyperspectral data and GOME-2 ozone data ensured an accurate representation in the IFS of the ozone hole associated with the vortex. The main vortex was accompanied by two less intense companions that lived about one month each and were also represented by the IFS. Similar events were also detected after the Canadian fire of 2017.

Understanding the ability of smoke clouds to self-organise into structures lofting themselves to high altitude is a new challenge for geophysical fluid dynamics. This ability is also a factor that increases the residence time of smoke plumes and their effect on the climate, which is comparable to moderate volcanic eruptions of the last decade.

For more details on the research study, see the Nature Communications Earth & Environment article by Khaykin et al. (2020), <https://www.nature.com/articles/s43247-020-00022-5>.



**Australian fire smoke in the stratosphere.** The smoke cloud observed by the CALIOP space-based lidar instrument on 31 January 2020 is shown in the left-most vertical cross-section. The cross shows the vortex vorticity centroid location in the ECMWF IFS analysis projected onto the satellite track. The other panels show the ECMWF IFS analysis for a vertical east-west cross-section through the vortex on the same day. The strong anticyclonic circulation and large temperature dipole are evident.

# GloFAS helps Bangladesh flood forecasters to predict monsoon flood

Sazzad Hossain (University of Reading, UK, and FFWC, Bangladesh), Christel Prudhomme (ECMWF), Hannah Cloke, Liz Stephens (both University of Reading)

The impacts of the 2020 monsoon in Bangladesh were devastating with more than 5 million people affected by the floods, 41 casualties and tens of thousands of people living in low lying areas evacuated to flood shelters along with their cattle. During the South Asian summer monsoon, floods are a frequent natural hazard in the Brahmaputra river basin in Bangladesh, but the type of flood that happens can vary significantly depending on the monsoon rainfall and basin hydrological characteristics. Flood forecasters for the Brahmaputra consider three very important questions: when will flooding commence during the monsoon period, how long will it last and will there only be one flood or many flood waves? Predicting flood timing and duration with a sufficient lead-time is an additional challenge.

The Global Flood Awareness System (GloFAS) is produced by ECMWF as part of the Copernicus Emergency Management Service (CEMS) and provides operational extended-range ensemble flood forecasts with a 30 day lead-time for major world river basins including the Brahmaputra in Bangladesh. The GloFAS team from

the University of Reading and ECMWF are working together with the Bangladesh Flood Forecasting and Warning Centre (FFWC) and humanitarian partners to improve flood early warning in Bangladesh under the UKRI/FCDO Science for Humanitarian Emergencies and Resilience (SHEAR) research programme, so that forecasts issued to government and stakeholders are as skilful and useful as possible. GloFAS is freely available through a dedicated web interface (<https://www.globalfloods.eu>) or via the Copernicus Climate Data Store. GloFAS aims to provide early warning information of upcoming floods with a long lead-time to support disaster managers or national institutes for flood preparedness and response actions.

## Chronology of 2020 floods

GloFAS forecasts showed a 10-day duration flood event for the end of June around 2 weeks ahead. Ten days ahead, the signal was even stronger, predicting a flood event exceeding the 20-year return period level associated with heavy rain. As predicted, the first flood wave on the Brahmaputra was observed between

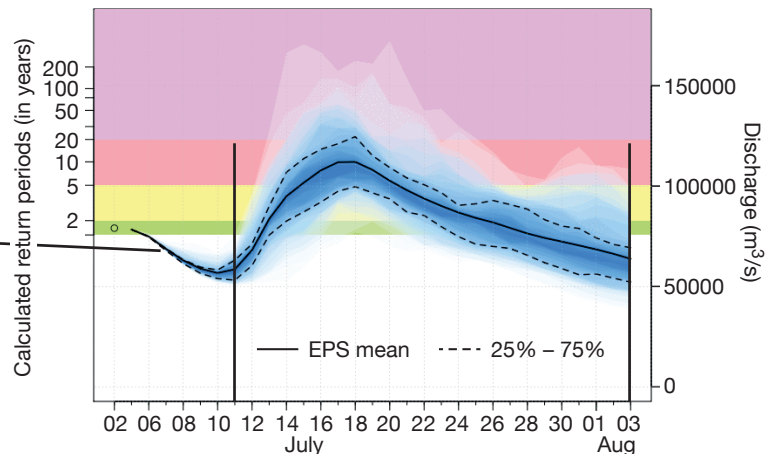
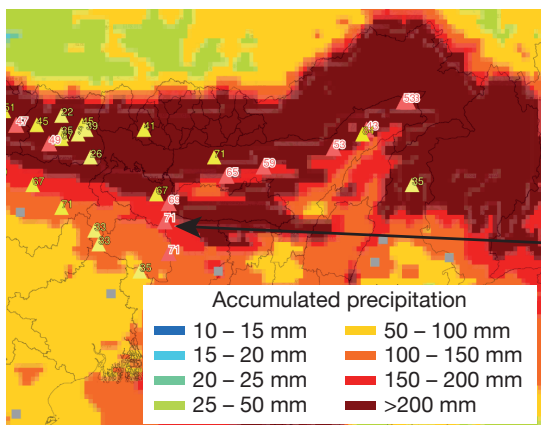


**Flood impacts in Jamalpur.** Flood-inundated house in the region affected by floods (Credit: Flood volunteer Abdul Mannan).

the 26 June and 7 July with flood levels peaking the 30 June. GloFAS also successfully predicted a second severe flood wave beginning on 11 July and reaching its peak on the 16 July (see figure). Overall, the two flood waves of the 2020 monsoon season in the Brahmaputra basin in Bangladesh lasted 35 days. GloFAS extended-range forecasts were able to predict the duration and timing of the flood waves accurately with a 10-day lead-time.

## Forecast communication

For the 2020 monsoon floods, the GloFAS forecast was communicated to different stakeholders from



**GloFAS river flow forecast.** GloFAS forecast on 4 July 2020. In the map showing rainfall levels over a 10-day period, reporting points (triangle and circle symbols) show river points with a predicted flood signal. In the GloFAS forecast, vertical lines show the potential start and end of the flood event (source: GloFAS, [www.globalfloods.eu](http://www.globalfloods.eu)).

national level to sub-national levels. National news media broadcast the risk of potential flooding as indicated by the Flood Forecasting and Warning Centre (FFWC) in Bangladesh. National and international NGOs, humanitarian agencies and development partners working in disaster response such as relief distribution have developed Forecast-based Financing (FbF)

methods to help their decision making ahead of flood events. This includes the Bangladesh Red Crescent Society (BDRCS), supported by the International Federation of Red Cross and Red Crescent Societies (IFRC), and three UN agencies (FAO, WFP, UNFP). On 4 July GloFAS forecasts indicated a high probability of floods 10 days ahead, which triggered a pre-

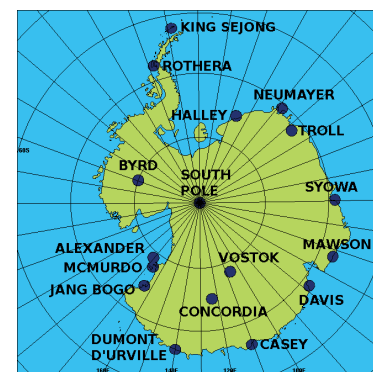
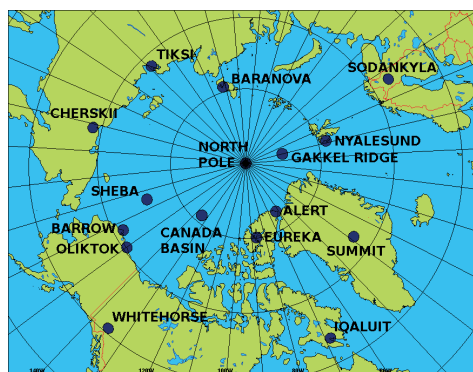
activation mode that released funds to in-country offices. Closer to the event the FFWC forecasts confirmed the imminent flooding, and cash and aid was provided to support vulnerable communities in the Bogura, Gaibandha, Kurigram, Jamalpur and Sirajganj districts, giving them the means to protect themselves and their livelihoods from the impacts of the floods.

## The YOPP site inter-comparison project

Jonathan Day (ECMWF), Gunilla Svensson (Stockholm University, Sweden), Barbara Casati (ECCC, Canada), Taneil Uttal (NOAA, USA)

A team of modellers, observationalists and data scientists collaborating under the umbrella of the World Meteorological Organization's Year of Polar Prediction (YOPP) have been working through the complex details of synergistically combining information from Arctic observatories and numerical weather prediction (NWP). They aim to further our understanding of polar meteorology and to assess and improve process representation in the polar regions. The project, known as YOPPsitMIP, is an international effort and has to date produced forecast data from eight NWP systems (including ECMWF's Integrated Forecasting System) at 41 polar terrestrial observatories. A number of these systems are also providing output at the MOSAIC ice camp as part of the MOSAIC-Near Realtime Verification Project. The dataset is archived at the YOPP portal, hosted by Met Norway.

Although the quality of weather forecasts in the Arctic is improving, it still lags behind the quality of forecasts in lower latitudes. Arctic regions pose specific challenges related to processes which are historically difficult to model (stable boundary layers, mixed-phase clouds, and atmosphere-snow-ice coupling). Moreover, so far there has been relatively little effort to evaluate processes in weather models using in-situ datasets from the terrestrial Arctic and Antarctic, compared to the situation in mid-latitudes. YOPPsitMIP aims to address this gap.



**Polar observatories.** Maps of polar observatories included in YOPPsitMIP.

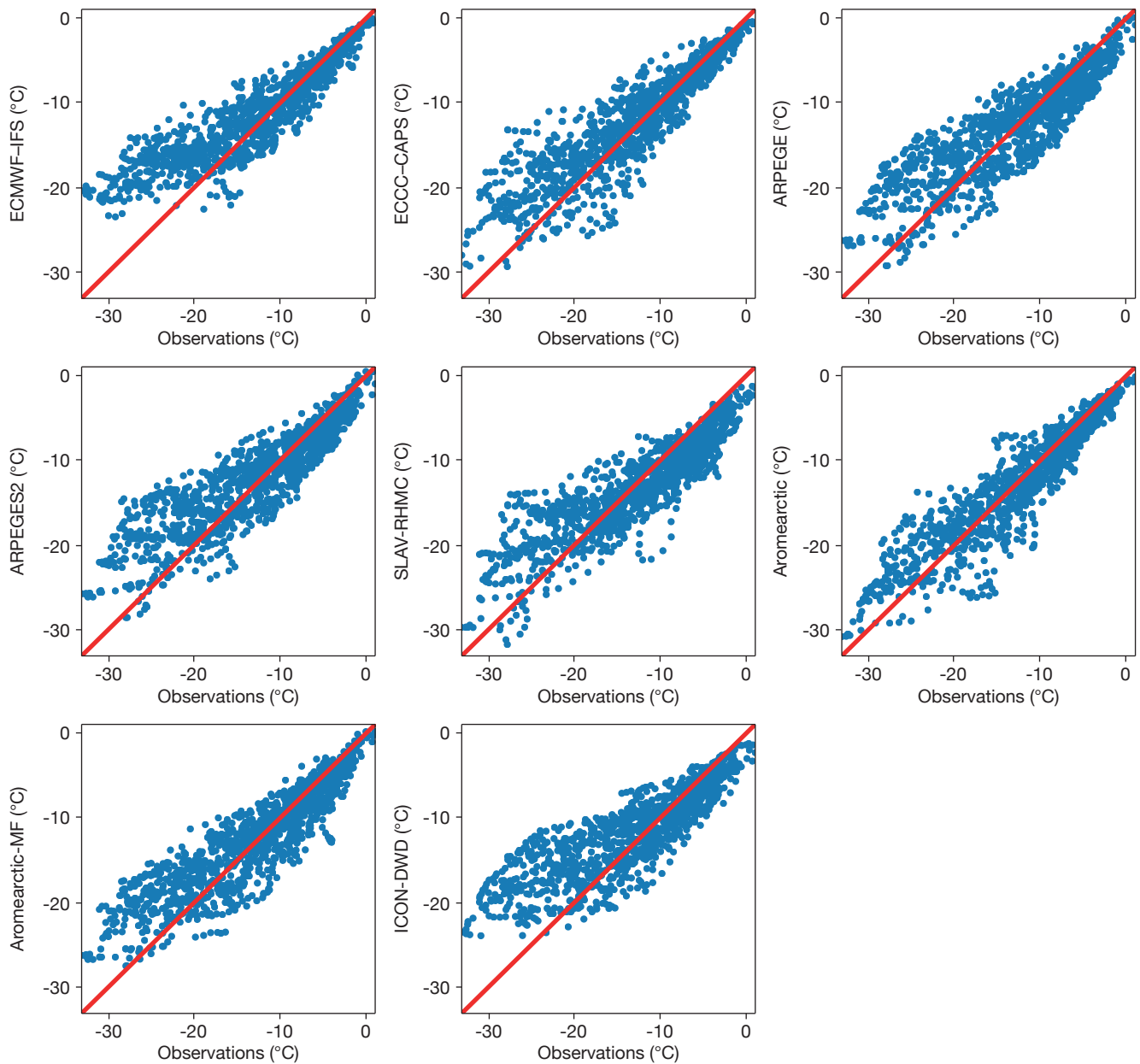
While the concept of model inter-comparison is not new, there are novel challenges associated with the YOPPsitMIP activity:

- (1) The focus is on coupled NWP models, assessing their performance at a process level in the polar environments. This requires the development of consistent time series at specific grid points, with high frequency to model time-step outputs from different NWP centres.
- (2) The observatory data, which includes variables originating from scores of instruments, researchers, institutions, archives and portals, need to be organised into consistent Merged Observatory Data Files (MODFs).

Initially efforts will focus on the YOPP special observing periods (SOP1: Feb–Mar 2018, and SOP2: Jul–Sep 2018, SOP–Southern Hemisphere: Nov–Feb 2018/19) and the MOSAIC

year (Sep 2019 to Sep 2020). The YOPPsitMIP dataset complements the ECMWF-YOPP dataset, which contains spatial fields, albeit at a lower temporal resolution.

An initial evaluation across the models already provides some interesting results. For example, most of the forecast systems exhibit a warm bias in extremely cold conditions. This can be seen in both northern Europe (as illustrated in the second figure) and northern Alaska. Finding common issues like this across models and attributing these to certain processes/parametrizations, which can then be tackled in community efforts, is a key theme. For example, in all the NWP systems shown, terrestrial snow is represented by a single thermal layer. Recent work at ECMWF, as part of the APPLICATE project, has shown that this bias is partly caused by this simple representation of the snow. Including a multi-layer snow model can improve, but not completely solve,



**Temperature forecasts and observations.** Hourly near surface temperature forecasts for day 1 at Sodankylä, Finland, compared to observations from (top left to bottom right): ECMWF–Integrated Forecasting System (ECMWF–IFS), Environment and Climate Change Canada–Canadian Arctic Prediction System (ECCC–CAPS), Météo-France ARPEGE version without variable sea-ice surface temperature (ARPEGE), Météo-France with variable sea-ice surface temperature (ARPEGES2), Russian Federal Service For Hydrometeorology and Environmental Monitoring (SLAV-RHMC), Met Norway (Aromearctic), Météo-France (Aromearctic-MF) and the German national weather service (ICON-DWD).

this error in the IFS. Understanding whether this is the case for all the contributing systems would obviously help inform model development choices across the community.

**Future plans**

The next steps for YOPPsiteMIP are to produce MODFs for each of the sites and to use these in a process-oriented evaluation of the forecasts. The NWP centres, including ECMWF, have been providing input into the design of

these files. This is designed to ensure a fair comparison with the forecasts themselves. However, producing standardised MODFs for the observatories is much more challenging than for the forecasts, since it requires bringing together a mixture of routine and research grade observations. A prototype MODF has been produced for Utqiagvik (formerly Barrow) Alaska by the US National Oceanic and Atmospheric Administration (NOAA), and a team

has been assembled to begin producing these for other sites according to this template. Once completed, it is expected that the MODFs produced for the polar observatories will provide a valuable resource for benchmarking NWP and climate models, from a process perspective, for many years to come. Further model evaluation using these is planned as part of upcoming projects, including ECMWF’s contribution to INTERACTIII.

# Using the EFI for water vapour flux at the UK Met Office Flood Forecasting Centre

Dave Cox (UK Met Office), David Lavers (ECMWF)

The Extreme Forecast Index (EFI) for water vapour flux became operational in Integrated Forecasting System (IFS) Cycle 46r1 in June 2019 (ECMWF Newsletter 160). The benefit of this EFI parameter is twofold: (1) potential to provide earlier awareness of extreme precipitation on the west coasts of mid-latitude continents than by using the EFI for precipitation; and (2) illustration of the synoptic-scale processes (atmospheric river activity) behind extreme hydrometeorological events. This article details the collaboration between ECMWF and the Flood Forecasting Centre (FFC) at the UK Met Office on this EFI parameter and its operational trial during the winter of 2019/20, and it introduces some useful guidance for its use and interpretation alongside other products.

## Daily tasks

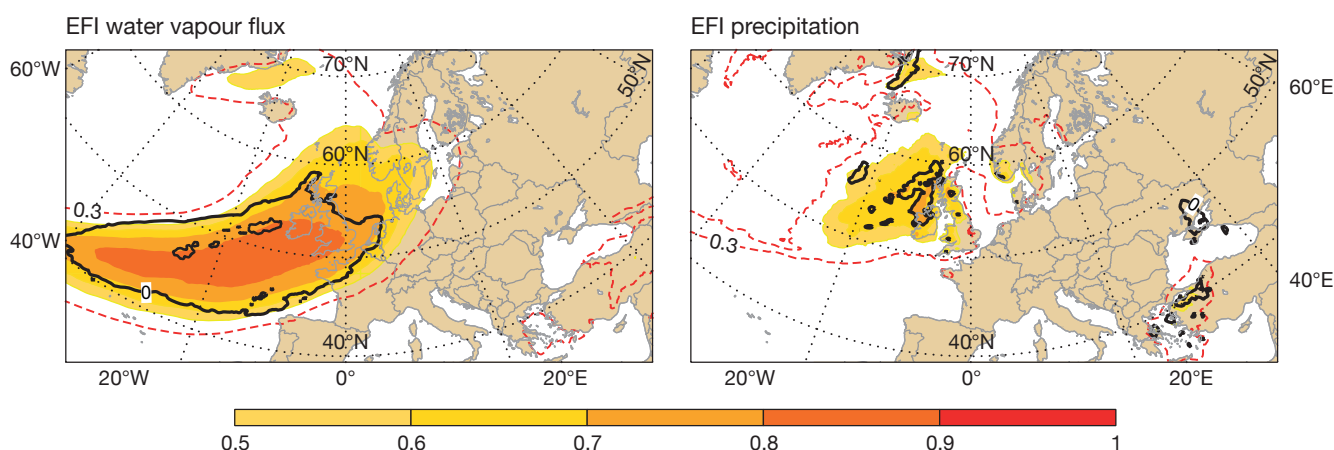
ECMWF scientists and FFC hydrometeorologists have discussed the forecast opportunities surrounding the EFI for water vapour flux in multiple meetings since 2016. Of most interest to the FFC is the possibility to have enhanced predictability of extreme events so they can give Category 1 and 2 Responders (such as the Environment Agency and Natural Resources Wales) additional time to prepare and respond to such events. Following a pre-operational

assessment in winter 2018/19, an operational trial was conducted in winter 2019/20. This coincided with a protracted period of unsettled weather and widespread flooding. Throughout the winter, a daily task was scheduled to evaluate the water vapour flux EFI fields and to monitor regions near the UK where the EFI exceeded 0.5 (this value signifies the possibility for extreme conditions). The focus was predominantly on forecast days 6 to 10, and the EFI was used by FFC hydrometeorologists as an additional decision-making tool when writing the Flood Guidance Statement.

An example of the useful guidance provided by the EFI for water vapour flux is given in the figure for Storm Dennis on 15 February 2020. A week after Storm Ciara, Dennis brought further widespread heavy and persistent rainfall to high ground across much of England and Wales, with the largest rainfall accumulations over the Brecon Beacons in south Wales. The water vapour flux EFI gave useful guidance at days 7–9, and particularly from day 7, for another large-scale rainfall event that, as it would be falling on mostly saturated catchments, had potential for significant flooding impacts. This was an earlier and stronger sign than that provided by the precipitation EFI.

## Lessons learnt

Lessons learnt from the trial include a number of useful guidelines for use of the EFI for water vapour flux from an operational perspective. It is first most appropriate to assess the EFI for water vapour flux and precipitation together to give FFC hydrometeorologists the best opportunity to understand the potential for rainfall/flood events. Second, during winter 2019/20, earlier indications of wet periods of weather (at day 6 and beyond) were found by using the EFI for water vapour flux compared to the precipitation EFI; moderate EFI values for water vapour flux were also occasionally seen on days 10–15. However, the EFI for water vapour flux was often rather too broad and, on occasions, shifted to the south on forecast days 6–9 compared to observed rainfall (and sometimes compared to the precipitation EFI). This southward displacement of the EFI signal was associated with a series of travelling lows. Third, the archetypal synoptic model for atmospheric rivers (ARs) in the UK is a mature, deep quasi-stationary low-pressure system near Iceland and an established high-pressure system over or near the Iberian Peninsula, the result being a strong southwesterly maritime flow from lower latitudes. In these situations, the distribution of the rainfall is likely to



**EFIs and Shift of Tails for water vapour flux and precipitation.** This figure shows the Extreme Forecast Index (EFI, shading) and Shift of Tails (SOT, contours) for water vapour flux (left) and precipitation (right) valid for 15 February 2020 on forecast day 7 (T+144 to T+168).

be more consistent with the position of the AR and clearly modulated over the western high ground. In contrast, users must note that the water vapour flux EFI will not produce a signal (indicative of large rainfall accumulations) from meteorological set-ups such as a slow-moving area of low pressure centred over England with persistent rain from a wrap-round occlusion.

The South Yorkshire flooding by the River Don on 7/8 November 2019 is an example where there was no EFI for water vapour flux signal in the run up to the event, although there was a weak EFI precipitation signal. Finally, there is a benefit in looking at the EFI for water vapour flux and precipitation at short range (days 1 to 3) as this can give the hydrometeorologist some confidence in

the potential for an unusual event.

ECMWF and the FFC will continue to work together to collaborate on the use of this EFI product. The FFC feedback provided is likely to be added to the ECMWF Forecast User Guide and the suggested improvements will be discussed in future meetings.

## Understanding how forecast users make decisions

Mark J. Rodwell, David S. Richardson (both ECMWF), John Hammond, Sara Thornton (both weathertrending)

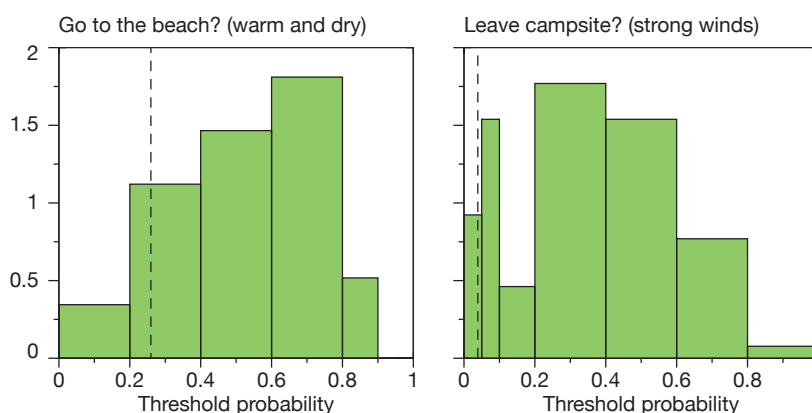
A Royal Meteorological Society ‘Live Science’ event, hosted at ECMWF, allowed us to investigate how forecast users combine objective forecast probabilities with their own subjective feelings when making weather-dependent decisions. Such decisions are integral to the overall utility of forecasts.

### Design of the study

For each of the 74 participants we identified the ‘threshold probabilities’ at which they decided to “go to the beach” in five days’ time with the possibility of warm dry weather, and at which they decided to “pack up and leave” a campsite in the face of potentially dangerous winds tomorrow. While making their decisions, participants were encouraged to elaborate mentally on each scenario as it might apply to them – who would they be with, what would they do, how far from home would they be, etc.? A key question in this study was whether users identify the threshold probability which optimises their expected feeling (or utility) about their decision. If they do this, then they are making their ‘Bayes Action’, and their feeling afterwards represents a ‘proper score’ of the forecast. Proper scores are fundamental in the development process of forecasting systems as they reward systems which issue ‘reliable’ (unbiased) probabilities, and which have better deterministic properties. If the users’ distribution of threshold probabilities is sufficiently consistent with their Bayes Actions, then there is the potential to develop scores which encourage user-oriented forecast system development.

### Results of the study

The distribution of participants’



**Participants’ threshold probabilities.** Distribution of the participants’ threshold probabilities for their decision to go to the beach in five days’ time with the prospect of warm dry weather (temperatures greater than 20°C and with less than 0.5 mm rain in 24 hr), and for the decision to leave a campsite with the prospect of dangerous winds tomorrow (sustained wind-speeds of more than 11 ms<sup>-1</sup> with stronger gusts). The dashed lines indicate the climatological frequency of each event.

threshold probabilities shows that the majority of them would plan to go to the beach if the probability of good weather exceeds about 0.7 (or 70%, see the first panel of the first figure). For the camping scenario (second panel), participants generally avoid dangerous wind at lower probabilities. Although our participants may be more familiar with probability information than the general user, we might assume that they represent the same range of feelings about a day at the beach or the prospect of dangerous winds. A vox pop of the general public actually reveals similar distributions of decisions. Hence a forecast presenter could perhaps interpret the probabilistic forecast for their audience: suggesting it would be worth making plans to visit the beach if the probability exceeded 70 or 80%. For the camping scenario, based on the threshold probability distribution, the presenter should certainly raise the alarm at a 30% probability.

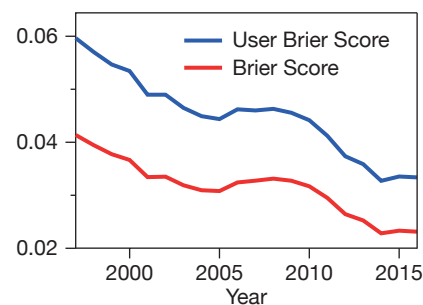
More detailed questioning indicates that, for the beach scenario, participants appear to be balancing the potential ‘Thrill’ of a nice day at the beach – “I love being on beaches, whatever the weather” – with the ‘Pain’ of a bad day at the beach and feelings about travel costs – “I hate sitting on the beach in the rain ... and with three kids it’s quite an expedition”. For the camping scenario, participants appear to be balancing the ‘Pain’ of curtailing a family holiday with the potential ‘Regret’ of putting loved ones in harm’s way: “With a low probability, I’d feel responsible for taking away my family’s fun. However, as a parent, I wouldn’t want to put very young kids at risk of flying branches. If it had been a very high probability and I hadn’t done anything I’d feel responsible”. However, a participant who chose a high threshold probability stated that “I don’t really go camping. If I’m already there,

I may as well stay as long as possible. A case of making it an adventure with the family pulling together to stop the tent being blown away". The reason for this apparent 'risk-seeking' behaviour may be a lack of first-hand experience – something that will be inevitable for many users when faced with a climatologically-rare, yet dangerous weather event. In recognition of this, a forecast presenter might decide that a dangerous wind warning should be issued at a probability lower than 30%, and authorities might also take more coercive action.

### The User Brier Score

We suggest that the obtained threshold probability distributions are more consistent with the participants' Bayes

Actions than, say, if we assumed a flat (i.e. uniform) or strongly peaked distribution. Certainly, the two distributions differentiate the scenarios in a reasonable way. We therefore assume that we can approximately equate the distribution of threshold probabilities with the distribution of the users' 'cost/loss ratios of feelings'. This allows us to calculate 'expense per unit loss'. We propose a 'User Brier Score' (UBS: see box) which measures the relative expense incurred by the user community as a whole, when provided with the forecast information. The UBS is asymptotically proper as the sample size increases, lies in the range [0,1], and reduces to the well-known Brier Score (BS) for the case when the users' distribution of cost/loss ratios is uniform. We use the UBS to score the ECMWF operational medium-range ensemble forecast for the period 1995–2018 using 'SYNOP' point observations for verification (locations between 50–60°N, June–August for the beach scenario and September–November for the camping scenario). This effectively scores the raw forecasts for our bivariate (temperature and precipitation) and extreme (wind) events at the location of the user. For both scenarios (the second figure shows the strong wind scenario), the UBS is higher than the BS, largely because the users' threshold distributions put less weight on high cost/loss ratios than does a uniform distribution. The general



#### User Brier Score and Brier Score.

The User Brier Score (blue) for the user community as a whole based on their indicated decisions in the face of potentially dangerous winds. The standard Brier Score is also shown (red). The curves have been smoothed with a five-year running-mean, the central year being indicated on the x-axis.

downward trend indicates reduced expense and thus improvement.

Much of the improvement, particularly for the campers, is due to a big reduction in 'complete misses' (where zero ensemble members predict the event, but there is a non-negligible outcome frequency). Complete misses remain a key issue, however, and this study suggests users would benefit from continued research into the modelling of extreme weather, and its likelihood when on the edges of the forecast distribution.

Further information can be found in Rodwell, M.J. et al., 2020, QJR Meteorol Soc., doi:10.1002/qj.3845.

#### User Brier Score (UBS)

$$UBS = \frac{\bar{E}_p - \bar{E}_o}{\bar{E}_{1-o} - \bar{E}_o}$$

where  $E_p, E_o$  and  $E_{(1-o)}$  are the 'expenses' incurred by a user if they took their Bayes Action when given: forecast probability  $p$ , a perfect forecast (knowledge of the outcome)  $o \in \{0,1\}$ , and the worst possible forecast  $1 - o$ , respectively. An overbar  $\bar{\phantom{x}}$  indicates the mean over a representative sample of forecasts, and a tilde  $\sim$  indicates the mean over the set of users.

## 2nd International Verification Challenge

Forecast verification is evolving beyond traditional metrics for basic weather variables to make use of many new sources of data to assess forecast quality. For example, data on weather-related damage and other societal impacts, social media, photos and other data from smart phones, and user-relevant variables such as energy output, crop yield, and so on, can all be used to evaluate forecasts and warnings. This additional evidence gives people greater confidence to use the forecasts in their decision making.

To encourage the development of verification approaches using new sources and types of observations, the World Meteorological Organization's Joint Working Group on Forecast Verification Research (JWGFVR) is conducting a challenge to develop and demonstrate new forecast verification metrics that make use of non-traditional observations.

New scores and visualisations are encouraged. The new approaches will support the WWRP High Impact Weather, Subseasonal to Seasonal Prediction (S2S), and Polar Prediction (PPP) projects.

The JWGFVR warmly encourages all interested researchers and practitioners to participate.

The deadline for entries is 30 April 2021. The winner will be announced in May 2021 and will receive all-expenses-paid attendance and a keynote address at the 8th International Verification Methods Workshop to be held in late 2021.

More information and an entry form are available at: <https://community.wmo.int/news/2nd-international-verification-challenge> or write to <mailto:verifchallenge@bom.gov.au>.

- Find new scores and visualisations
- Use non-traditional observations
- Develop a new verification approach

# The life of GLAMEPS

Trond Iversen, Inger-Lise Frogner (both Norwegian Meteorological Institute), Xiaohua Yang, Kai Sattler (both Danish Meteorological Institute), Alex Deckmyn (Royal Meteorological Institute of Belgium)

GLAMEPS (Grand Limited-Area Model EPS) was a pan-European multi-model ensemble prediction system (EPS) for reliable short-range forecasts developed by the HIRLAM and ALADIN consortia. The development started in 2005, and the system was run as one of the first time-critical applications at ECMWF from 2011 to 2019 with an upgrade in 2014. The skillful ECMWF staff was crucial for the implementation and production of GLAMEPS. It included a hierarchy of emergency procedures in real time, and GLAMEPS-staff were contact

points in cases when manual interventions were necessary. Computer resources were dedicated by HIRLAM and ALADIN countries from their national ECMWF quotas.

## Basic concepts

GLAMEPS aimed to provide predictions up to 2–3 days ahead which accounted for initial state and model inaccuracies and addressed risks of high-impact weather. The system that became operational achieved better probabilistic

verification than ECMWF’s ensemble forecasts (ENS) for most near-surface weather parameters (see figure for an example).

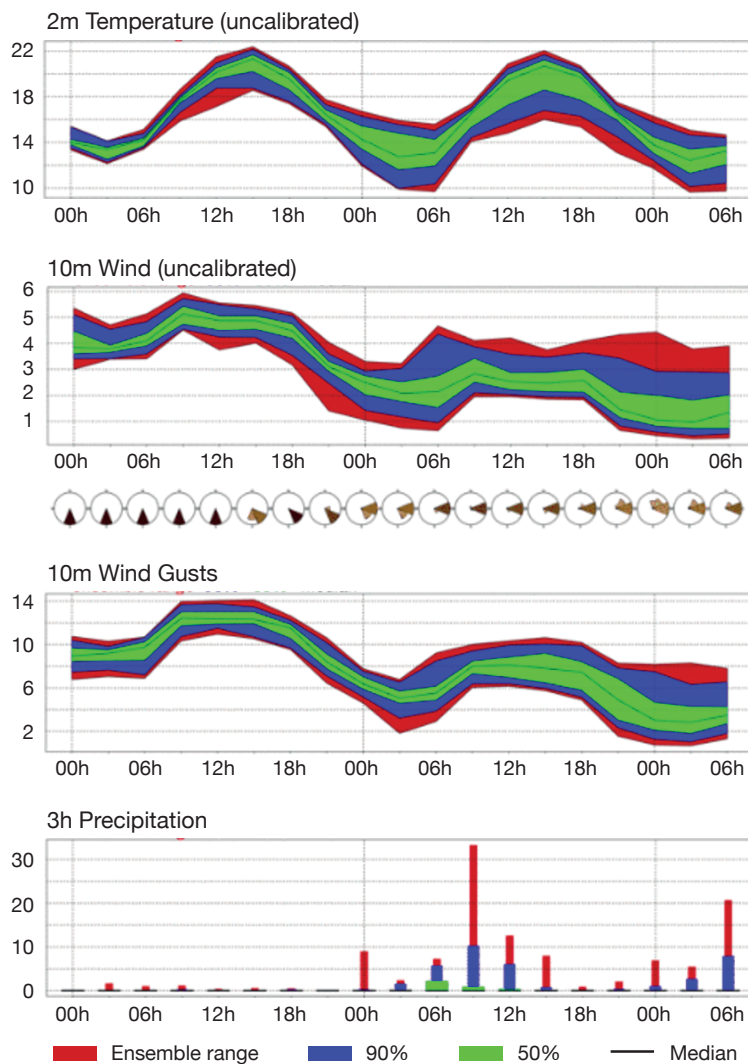
The system made use of a few different limited-area numerical weather prediction models, which formed the basis of alternative control forecasts as well as different sets of alternative ensemble forecasts. There was an emphasis on accounting for forecast uncertainty originating from processes at the ground surface. In addition to the higher level of spatial detail than in ENS, the multi-model approach proved valuable for improving the forecasts relative to those produced by ENS for the short range.

## Pre-operational GLAMEPS

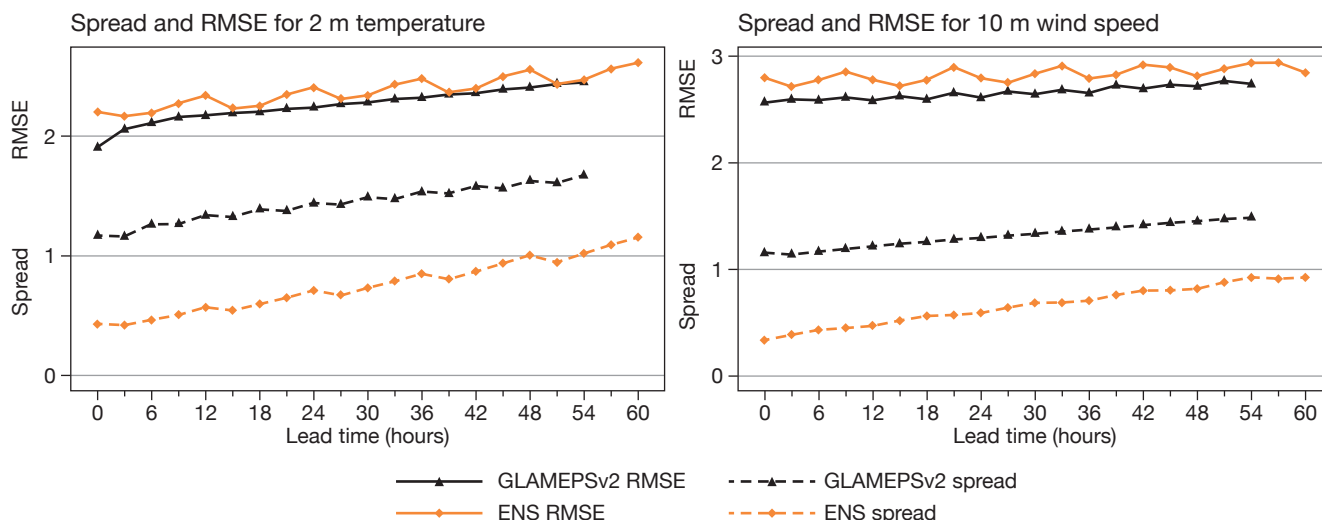
This prototype was run twice daily up to 42 hours for a seven-week winter period. The results were analysed and published scientifically. The 52 members of GLAMEPS\_v0 consisted of three control forecasts, four different models, and EuroTEPS, a model with stochastic physics. EuroTEPS was a version of ENS with perturbations spatially targeted for Europe that was run on behalf of HIRLAM and ALADIN with the same resolution as ENS at that time (~55 km). The horizontal mesh width was ~13 km for the LAM models. The HIRLAM model used two parametrizations of deep convection, which also produced two control runs based on parallel data assimilation (3D-Var). The third control run was from EuroTEPS, while ALADIN downscaled EuroTEPS members.

The forecasts by GLAMEPS\_v0 scored better than ENS with respect to ensemble calibration, forecast reliability and information content, and potential economic value. The multi-model approach was important for the improved quality. Since replacing EuroTEPS with ENS degraded the forecasts only slightly, it was decided to use ENS operationally as the global model.

GLAMEPS meteogram, Reading, 1 July 2019



**GLAMEPS meteogram.** Example of a GLAMEPS meteogram showing forecasts of 2-metre temperature, 10-metre wind, 10-metre wind gusts and 3-hour precipitation.



**Verification of GLAMEPS and ENS.** Ensemble spread and root-mean-square error (RMSE) of ensemble mean for temperature at 2 m (in °C) and wind speed at 10 m (in m/s) in February 2015 of GLAMEPS compared to ENS. Notice that both the RMSE and its deviation from the spread are smaller in GLAMEPS.

### GLAMEPS 2011–2013

This first operational version used all 51 members of ENS, either directly or as boundary and initial perturbations, and in addition the high-resolution forecast from ECMWF (HRES).

The model domain was increased by 30% with higher horizontal resolution (~11 km), and separate ground surface data assimilation cycles were run for each ensemble member from the HIRLAM and ALADIN-ALARO models. The latter was motivated by the increased potential predictability of weather features forced by the ground surface.

To optimize the timely use of ENS in ECMWF’s own production schedule, hours 06 and 18 UTC were the base times for the 54 h ensemble forecasts, which added up to 54 members. A selection of standard probabilistic maps and EPS-meteograms were provided, along with raw data (see figure for an example).

### GLAMEPS 2014–2019

The upgrade in 2014 included increased horizontal resolution (~8 km)

and up to 60 h forecasts produced four times per day (00, 06, 12, and 18 UTC). Ensemble members from ENS were no longer part of the multi-model ensemble but provided perturbations of initial and lateral boundary conditions.

The multi-model approach had four sub-ensembles, each with six new members produced six-hourly. The four sub-ensembles used separate model configurations, two of HIRLAM and two of ALADIN-ALARO. Each model configuration also produced one new control every six hours. By combining the new 24 ensemble members with the 24 from the previous base time, 4 control runs and 48 alternative ensemble members were available six-hourly. Stochastic perturbations of physics tendencies were included in the HIRLAM model.

The upgrade enabled probabilistic forecasts with increased spatial resolution, earlier delivery, more frequent updates, and extended forecast range. The added value over corresponding products from ENS was maintained operationally.

Extensive verification with the HARP validation package developed for GLAMEPS revealed that an important contribution to the skill enhancements of GLAMEPS was the combination of models with comparable forecast quality. Lagging of ensemble perturbations also enhanced the skill. Corresponding single model ensembles produced insufficient internal spread, although it was improved by the stochastic physics tendencies.

### Conclusion

GLAMEPS production stopped in 2019. The HIRLAM and ALADIN consortia saw the need to pursue even higher resolution EPS for the very short range, appreciating that very small-scale phenomena often are important for the development of extreme weather. The success of GLAMEPS, as well as its limitations, inspired the ongoing operational and experimental work on convection-permitting EPS in sub-European domains, implementing many of the successful system elements developed for GLAMEPS.

## New observations since July 2020

The following new observations have been activated in the operational ECMWF assimilation system since July 2020.

Observations	Main impact	Activation date
Wind observations from MODE-S aircraft data	Tropospheric wind	28 July 2020

## How to make use of weather regimes in extended-range predictions for Europe

Christian Grams (Karlsruhe Institute of Technology), Laura Ferranti, Linus Magnusson (both ECMWF)

**T**he concept of weather regimes was introduced in weather forecasting about 70 years ago (Rex, 1951). It is based on the idea that the large-scale atmospheric circulation can in practice be represented by a finite number of possible atmospheric states that manifest themselves in quasi-stationary, persistent, and recurrent large-scale flow patterns. Because the actual instantaneous weather differs from day to day and evolves continuously with time, classifying weather maps in a finite number of slowly varying states is not a simple task. There are many ways to define weather regimes. Referring to the property of recurrence in the sense of the most frequent patterns in a climatological period, cluster analysis is nowadays the most common approach to identify regimes. Based on quasi-stationarity and persistence, weather regimes represent, in a statistical sense, the states for which the large-scale flow pattern resides for an extended period (a week to a month). This definition offers an intuitive description of the weather variability. Weather regimes then describe the long-lived, large-scale circulation pattern perturbed by individual highs and lows. In this article we will discuss a few different regime definitions for the Euro-Atlantic region with different levels of complexity and show examples of useful visualisations, using ECMWF forecasts as a basis.

### Weather regimes

The real atmosphere is not discrete with its state space limited to a low number of states to reside in, but several potential stable states might exist depending on the current flow situation. There are various weather regime definitions which account for this large-scale flow variability but share common regime characteristics: their large spatial extent affecting continent-scale regions and their persistence of typically longer than 10 days. Although the existence of weather regimes over the Euro-Atlantic sector depends upon the midlatitude dynamics, the presence of external forcings, such as tropical heat anomalies or fluctuations of the stratospheric polar vortex, can modulate their frequency of occurrence.

The persistence of the weather regimes and their sensitivity to external forcings give rise to increased predictability at the extended range, when the predictability of synoptic perturbations declines. But at the same time, it raises the forecast challenge to correctly represent weather regimes and predict transitions from one regime to another in numerical models (e.g. Ferranti et al., 2015; Grams et al., 2018).

Beyond the fact that weather regimes can be regarded as physical modes with specific life cycles and transitions, another intriguing property of the regime concept is the connection of weather regimes to surface weather and weather extremes. Specific regimes particularly provide the environmental conditions conducive to large-scale cold spells in winter, heat waves in summer, and widespread heavy precipitation or thunderstorm activity. They also affect the generation of renewable energies on sub-seasonal time scales (e.g. Ferranti et al., 2019; Grams et al., 2017).

Despite the challenge of weather regime representation in numerical models, the conceptual model of regimes has proven to be a useful way to extract forecast information on the extended range, especially in ensemble forecasting. Still, with the huge amount of data from an ensemble system, it is necessary to condense the information in some way. One way to do this is to identify and visualise the dominant regime of the day in each ensemble member.

The difficulty in doing so is how to define the regimes and how to visualise them. For the regime definition there are a number of degrees of freedom: region, number of regimes, life-cycle definition, seasonality etc., and each is relevant so that there is no unique regime definition covering all use cases.

### How to construct regimes

Weather regimes aim to describe recurrent, quasi-stationary, and persistent states of the atmospheric circulation in a specific region. Since the advent of reanalysis data, identifying the leading modes of variability and clustering has become most common (e.g. Michelangeli et al., 1995). The leading empirical orthogonal functions (EOFs) on a large-scale flow field are computed: typically anomalies of geopotential height at 500 hPa or mean sea level pressure. This is

followed by a clustering of the leading EOFs which attributes each analysis time to a specific cluster in the EOF phase space and allows the computation of the pattern of the cluster mean anomaly in physical space. Prior to applying the EOF, analysis data is often low-pass filtered (typically 10 day cut-off) to remove synoptic-scale variability.

For the Euro-Atlantic sector, four regimes have been shown to be optimal for seasonal regime definitions. Seasonality in the amplitude of the considered large-scale flow anomaly, which is usually less in summer compared to winter, is another problem to deal with. To tackle this, regimes are often defined separately for different seasons, or consecutive 3-month periods, and blended into each other. However, summer and winter regimes differ substantially and regime behaviour in individual transition seasons often fits in either group so that there is no unique regime definition for spring and autumn. To address this problem, we here also use a novel regime definition accounting for seasonal variability by identifying an optimal number of seven year-round regimes in 500 hPa geopotential height anomalies, which are normalised to remove the seasonality in the amplitude.

Finally, even more refined regime definitions exclude days with only a weak projection into a regime by applying a persistence criterion (often at least 5 days) and further criteria to define sophisticated regime life cycles with objective life cycle stages, such as regime onset or decay. In this article we discuss the depiction of weather regimes in three such different definitions for the Atlantic-European region with increased level of complexity:

(1) The mere attribution in EOF1/2 space (see Ferranti et al., 2019). EOF1 corresponds to the two phases of the North Atlantic Oscillation (NAO), and EOF2 corresponds to the East Atlantic pattern, similar to a Scandinavian blocking in winter (BLO), so that the EOF1/2 space is also denoted as  $NAO_{\pm}/BLO_{\pm}$ .

(2) The classical four weather regimes based on EOF-clustering and regime attribution in EOF space, excluding weak projections into the EOFs, (denoted 4WR, see Ferranti et al., 2015). These reflect the two phases of the NAO complemented by the Atlantic Ridge and European/Scandinavian blocking regime. Two sets of 4WR are considered in operational forecasting at ECMWF, one valid for the cold period (October to April) and the other for the warm period (May to September). For the daily attribution, the 4WR spatial patterns are then adjusted to take into account the seasonal signal. A given regime is assigned only if the minimum distance between the anomalies and any of the 4WR is within an ‘average value’ and if the distance is significantly different from the others.

(3) A year-round definition of seven weather regimes based on EOF-clustering but with the regime attribution based on the projections of the instantaneous 10-day low-pass filtered 500 hPa geopotential height anomaly in the seven cluster mean fields in physical space and a sophisticated life-cycle definition (denoted 7WR, see Grams et al., 2017). The seven regimes reflect the 4WR patterns but allow three variants of cyclonically dominated regimes to be distinguished instead of NAO positive alone, and the four blocked regimes can distinguish blocking over Europe or Scandinavia.

## Variance explained by regime definitions

In order to effectively condense forecast information, a regime definition must explain as much as possible of the variance in the atmosphere over a specific region with a few patterns. Therefore, we first discuss the variance explained by the leading 2 and 20 EOFs based on climatological variability as well as the 4WR seasonal and the 7WR year-round definition with data from 20 November 2019 until 11 March 2020 (Figure 1). The 10-day running mean removes synoptic variability in accordance with the use of 10-day low-pass filtered

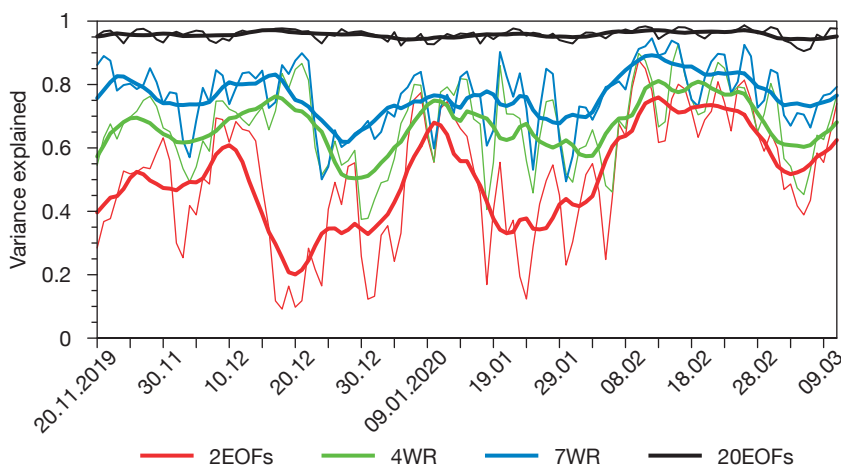


**FIGURE 1** Variance explained by the leading 2 and 20 EOFs, and the phase space spanned by the 4WR and 7WR definitions in winter 2019/20. Thin lines show daily values, bold lines the 10-day running mean.

data for the 4WR and 7WR definitions. The computation of the variance is explained in Box 1.

Much of the variance is explained already by the leading 2 EOFs (red), with on average 50% during the plotted period. Increasing the number of EOFs to 3 and 7 would increase the explained variance to around 65% and 80% respectively (not shown), while gradually reducing the temporal variability in explained variance. Likewise, the more complex 4WR and 7WR definitions explain on average 67% and 77% of the variance, respectively, both with similar temporal variability. The temporal variability in the explained variance is less for the more complex regime definitions with additional clustering compared to the raw EOFs. In particular during a period in the middle of December 2019, 2 EOFs explained only 20–30% of the variance compared to 60–80% by the other definitions. On the other hand, during the second half of February 2 EOFs explained more than 70% of the variance while 7WR explained more than 90%. Thus, while the 2 leading EOFs already explain a substantial fraction of variance, adding more complexity helps explain the bulk of variance during different flow situations. 7WR seems to be a good compromise to explain about 80% of the variance during most times, while the 7 possible states remain manageable.

## Examples of regime depiction in analysis

Figures 2 and 3 show the projections into each regime from the three different regime definitions in extended winter 2019/2020 (20 November 2019 to 10 March

### a Computing explained variance

The variance is computed with the following procedure: (1) use the Gram-Schmidt method to create an orthogonal base for each set of regimes, and (2) calculate the sum of the variance explained by the projection of the daily anomaly onto each orthogonal field. The sum of the variance is divided by the total variance of the daily field. The variance explained by the leading 20 EOFs (black in Figure 1) serves as a benchmark and is above 0.95 for almost the entire period.

2020) based on operational analysis data. As mentioned above, a 10-day low-pass filter has been applied to the projection time-series. For the 4WR regime definition, the present regime is determined by the regime with the highest positive projection coefficient in EOF space and weak projections are assigned to no regime. For the 7WR, the present regime is determined based on a life-cycle definition in physical space and requiring at least 5-day persistence.

Before discussing the results, the reader should be reminded that the end of winter 2019/2020 was very mild in north-western Europe with prevalent positive NAO conditions (see also Magnusson et al., 2020). This is apparent in all regime definitions, with a dominance of

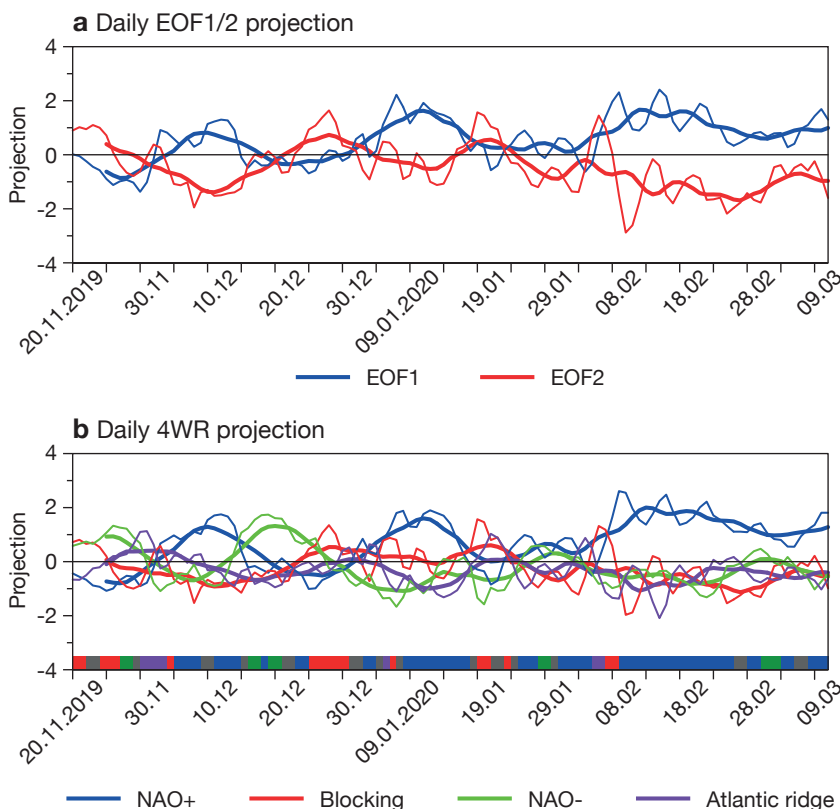


**FIGURE 2** Normalised projection of unfiltered 500 hPa geopotential height from operational analysis into (a) the first and second EOF and (b) the 4WR definition in winter 2019/2020. For 4WR we additionally show the daily attribution based on the distance to the cluster mean in EOF phase space with grey attributed to no regime.

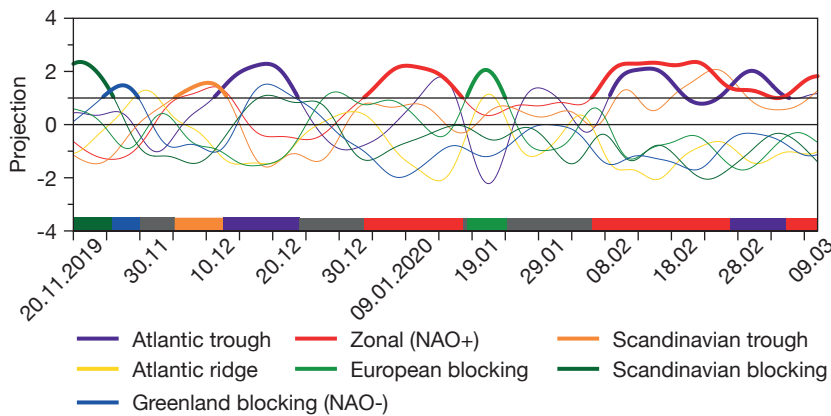


**FIGURE 3** Normalised projection of 10-day low-pass filtered normalised 500 hPa geopotential height into the 7 year-round regime life-cycle definition (7WR) in winter 2019/2020. Coloured lines show projection, bold lines indicate active regime life cycle with at least 5-day persistence. The bottom coloured bar shows the attributed regime (active life cycle and maximum projection) with grey attributed to no regime. Note that the attributed regime might not be dominant for 5 days as simultaneous life cycles are possible.

EOF1 in the NAO±/BLO± definition (Figure 2a), NAO+ in the 4WR (Figure 2b), and the cyclonic-type regimes (Atlantic trough, zonal, Scandinavian trough) in the 7WR (Figure 3).

The most persistent period took place through February into March, during which all regime definitions explained more than 70% of the variance (see discussion of Figure 1 above). During this period, the leading 2 EOFs were sufficient to explain most of the variance over the Euro-Atlantic area. However, 7WR gave the additional information of a slightly southward shifted storm track with the detection of a concomitant Atlantic trough regime in early March.

In contrast to the good agreement between the different definitions in February, there is a difference in the conveyed message in December. During this period a trough was present west of the British Isles, resulting in stormy conditions. Here the NAO±/BLO± definition failed to explain the variance as the projections onto the leading 2 EOFs were low. At the same time 4WR switched from NAO+ to NAO-, as it could not resolve the slight southward shift of the cyclonic pattern. However, the 7WR definition was able to identify this shift indicating Atlantic trough. In that case merely thinking of NAO- as a cold, calm regime in Europe is misleading, as the actual Atlantic trough indicates a stormy period with a strong southward shifted storm track. Moreover, in early December prior to the southward shift of the storm track and transition into NAO-/Atlantic trough in the 4WR/7WR definitions, the dominant projection into the Scandinavian trough for 7WR indicates that the cyclonic activity was further East than in the classical NAO+/zonal regime.

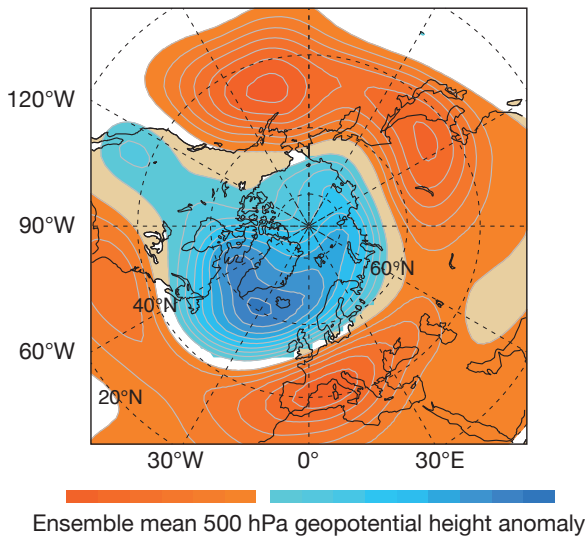
## Examples of forecast products

An important aspect of how to get the most information from the forecasts is how to visualise the products. Regime forecasts are a way to condense the amount of information. In this section we are illustrating different ways to visualise regime forecasts.

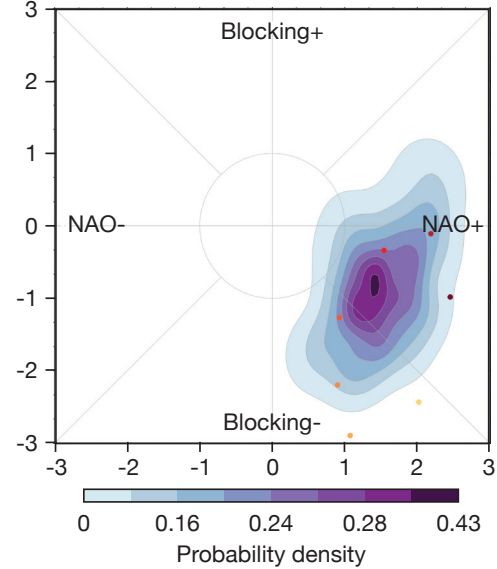
In Figure 4 we show examples of products from the same ECMWF extended-range forecast, initialised on 30 January 2020, which was a week before the onset of the positive NAO regime in all definitions that lasted for the rest of February. This forecast was also discussed in ECMWF Newsletter 163 (Magnusson et al., 2020). The first panel shows the ensemble mean anomaly of 500 hPa valid for 10–16 February (Figure 4a). The forecast had a strong negative anomaly over the north-eastern Atlantic and a positive anomaly to the south, which is the signature for a positive NAO. The next panel visualises the NAO±/BLO± definition showing the 2-dimensional distribution of daily projections of all ensemble members in the space spanned by the two leading EOFs (Figure 4b). The advantage of having two orthogonal regimes is that the forecasts can be visualised in such a phase diagram. Here we see that the product clearly indicates the state of a combination of the positive phase of EOF1 (NAO positive) and a negative phase of EOF2 (trough over Scandinavia). This very simple description of the forecast atmospheric evolution can be very effective in situations like this, in which the two leading EOFs already explain most of the variance, while other situations require a higher level of complexity (cf. discussion of Figure 1 above).

The two bottom panels (Figure 4c,d) show the regime forecasts where the dominating regime is detected for each ensemble member, with the size of each colour bar representing the probability for each regime and the x-axis representing the forecast length. The top plot is for 4WR and the bottom one for 7WR. This type of plot gives an overview of the ensemble distributions among the regimes and also the time evolution, but the drawback is that the categorical selection of regimes can hide information. Both regime forecasts correctly predict the final onset of an NAO+/zonal regime around 8 February. The visualisations shown in Figure 4a-c are freely accessible as official forecast products in the ECMWF charts catalogue (<https://www.ecmwf.int/en/forecasts/charts>). To complement the categorical product with continuous information about the actual

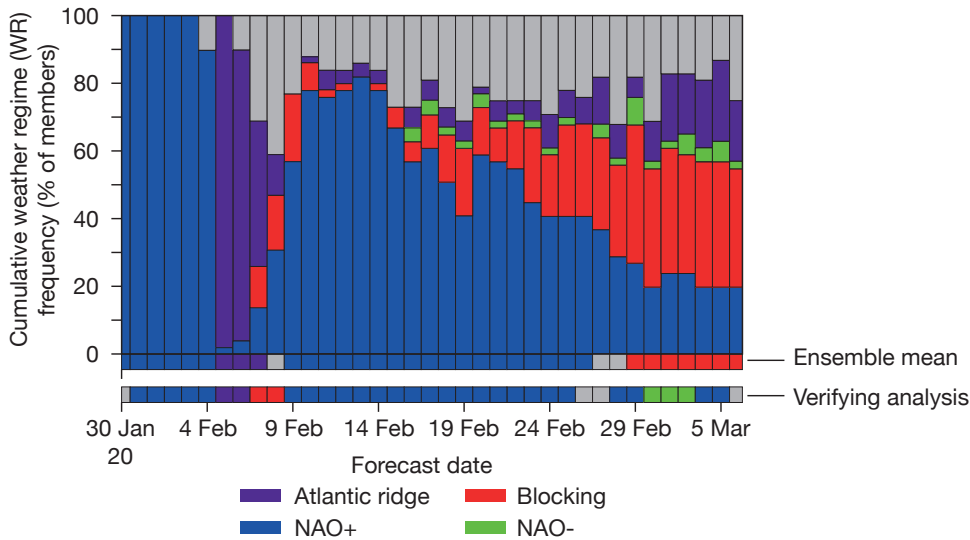
**a** Ensemble mean forecast, day 12–18



**b** Ensemble density of projection



**c** 4WR ensemble frequency



**d** 7WR ensemble frequency

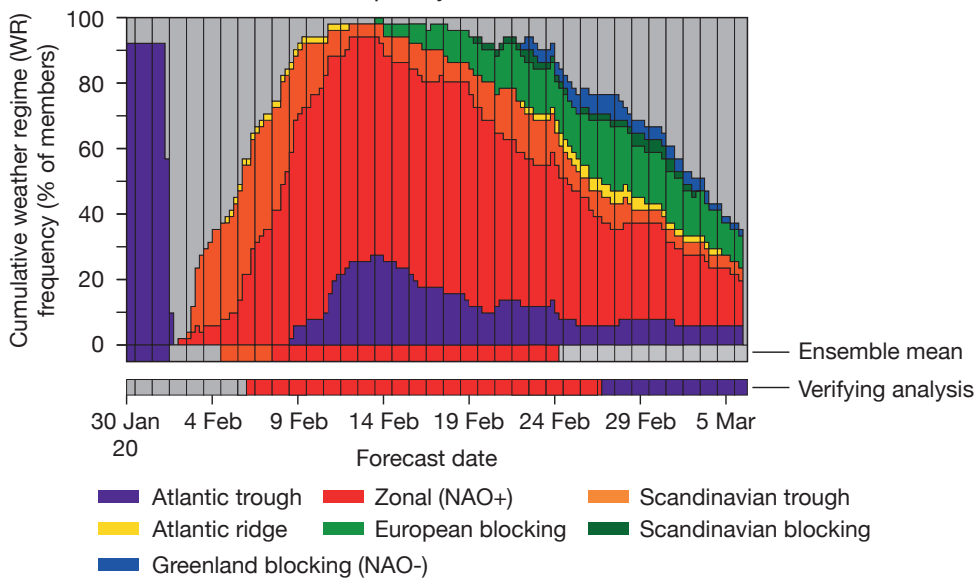


**FIGURE 4** Different visualisations of extended-range forecast initialised on 30 January 2020, showing (a) ensemble mean 500 hPa geopotential height anomaly for week 3 (valid 12–18 days after initialisation), (b) ensemble density of projection in NAO±/BLO± space for week 3, with the dots marking the daily values of the verifying analysis (yellow = first day to brown = last day), (c) categorical weather regime probability in ensemble for 4WR definition (daily data) and (d) categorical weather regime probability in ensemble for 7WR definition (6-hourly data). Additionally, the ensemble-mean attribution and the verifying analysis are shown.

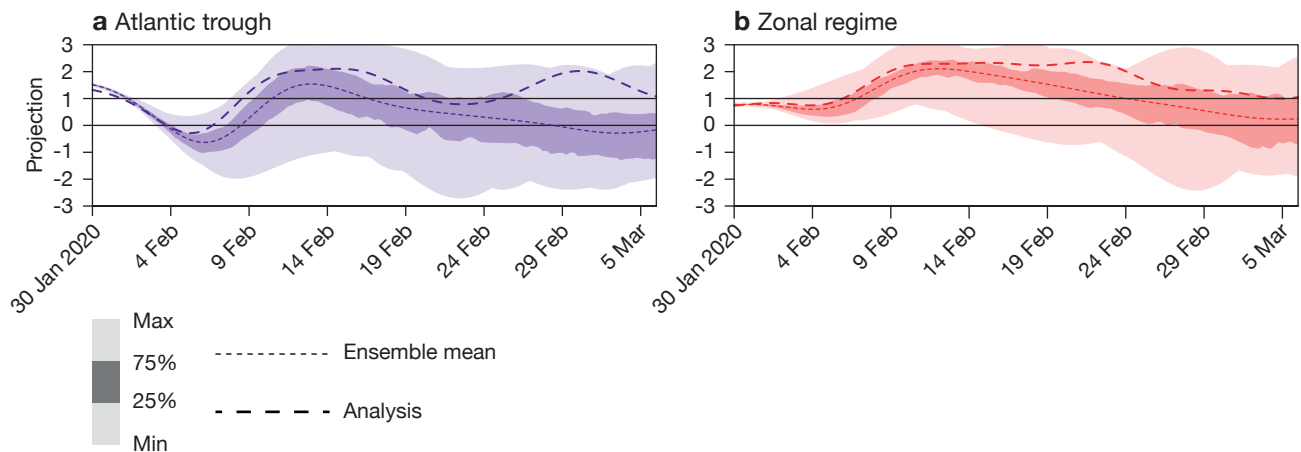


**FIGURE 5** Ensemble distribution of continuous weather regime index (normalized projection) in (a) the Atlantic trough of the 7WR definition and (b) the zonal regime of the 7WR definition. Light colours indicate the range of min/max projection, darker colours the interquartile range, short dashed line the ensemble mean projection and long dashed line the projection of the verifying analysis.

strength of the regime projection in the forecast, Figure 5 shows the time evolution of the ensemble distribution of the normalized projection for two of the regimes in 7WR. In the example situation it reveals that after the onset of the zonal regime, the projection into Atlantic trough remains concomitantly high, which reflects a slight southward shift of the storm track compared to a classical positive NAO.

## Summary

This article illustrated different ways to condense forecast information for the extended range with the help of weather regimes. We argue that using different regime definitions is a way to deal with flow-dependent predictability and better assess the current forecast skill horizon. We discuss a range of forecast products all based on weather regimes but each with a different level of complexity. While simple forecast products based on NAO±/BLO± projections or categorical attribution of ensemble members provide a quick overview, complementing this with continuous forecast information in terms of regime projections is a way to avoid misinterpretations in suspicious situations (e.g. the slight southward shift of the storm track in February 2020 or the putative transition from NAO+ into NAO- in December 2019). ECMWF has today operational products based on NAO±/BLO± and 4WR accessible via the charts catalogue (Figure 4b and 4c). The 7WR products are for now available as test products at the Karlsruhe Institute of Technology (KIT). Using such products in a routine way would help forecasters gain experience in regime behaviour and their impact on surface weather (e.g. cold spells, see Ferranti et al., 2019) on sub-seasonal time scales.

## Further reading

**Ferranti, L., S. Corti & M. Janousek**, 2015: Flow-dependent verification of the ECMWF ensemble over the Euro-Atlantic sector. *Q.J.R. Meteorol. Soc.*, **141**, 916–924, doi.org/10.1002/qj.2411.

**Ferranti, L., L. Magnusson, F. Vitart & D.S. Richardson**, 2019: A new product to flag up the risk of cold spells in Europe weeks ahead, *ECMWF Newsletter No. 158*, 15–20.

**Grams, C.M., R. Beerli, S. Pfenninger, I. Staffell & H. Wernli**, 2017: Balancing Europe's wind-power output through spatial deployment informed by weather regimes, *Nature Climate Change*, **7**, 557–562, doi.org/10.1038/nclimate3338.

**Grams, C.M., L. Magnusson & E. Madonna**, 2018: An atmospheric dynamics perspective on the amplification and propagation of forecast error in numerical weather prediction models: A case study. *Q.J.R. Meteorol. Soc.*, **144**, 2577–2591, doi.org/10.1002/qj.3353.

**Magnusson, L., F. Vitart & D.S. Richardson**, 2018: How far in advance can we predict changes in large-scale flow leading to severe cold conditions over Europe? *Q.J.R. Meteorol. Soc.*, **144**, 1788–1802, doi.org/10.1002/qj.3341.

**Magnusson, L., L. Ferranti, D. Lavers & F. Wetterhall**, 2020: Forecasting February's wet and stormy weather in parts of Europe, *ECMWF Newsletter No. 163*, 2–3.

**Michelangeli, P.-A., R. Vautard & B. Legras**, 1995: Weather Regimes: Recurrence and Quasi Stationarity, *J. Atmos. Sci.*, **52**, 1237–1256.

**Rex, D.F.**, 1951: The Effect of Atlantic Blocking Action upon European Climate, *Tellus*, **3**, 100–112, doi.org/10.3402/tessusa.v3i2.8617.

## CAMS contribution to the study of air pollution links to COVID-19

Vincent-Henri Peuch

**F**rom the early days of the COVID-19 pandemic, air pollution has emerged as an area of strong scientific and general public interest.

Air pollution has indeed been one of the most visible markers of the effect of lockdown measures. This has taken the form of a substantial observed decrease in the concentrations of certain pollutants like nitrogen dioxide (NO<sub>2</sub>) or fine Particulate Matter PM2.5 and PM10 (particles finer than 2.5 micrometres and 10 micrometres respectively). In particular, the measurements of the Copernicus Sentinel-5P TROPOMI satellite instrument, as reported by the Copernicus Atmosphere Monitoring Service (CAMS), the Royal Netherlands Meteorological Institute (KNMI) and the European Space Agency (ESA), have had a prominent place in the media. They showed fairly abrupt changes in different parts of the world as restriction measures were enforced or lifted. CAMS data have also been used in epidemiological studies and have been supporting the World Meteorological Organization's Global Atmospheric Watch programme in organising international efforts.

### Initial response

Initially, interpretation of lockdown effects on anthropogenic emissions has been done in a fairly crude way, by simply comparing the satellite-derived

pollutant amounts in 2020 with the ones observed for the same period of the year in 2019 and other recent years. Such studies have also been carried out similarly with surface observations. As can be seen in Figure 1, which presents CAMS daily surface analyses of NO<sub>2</sub> together with information on the dates when lockdown or restriction measures were in place for the city of Barcelona, the naïve interpretation of concentration changes by a reduction in emissions can be deceptive. Indeed, one can see in this example that, more than a month before any restriction measure was taken, 2020 levels of NO<sub>2</sub> were noticeably lower than in the three previous years. This can be easily understood because the month of February 2020, as shown by the Copernicus Climate Change Service (C3S), was exceptionally warm. The result was in particular higher than normal planetary boundary layer heights across most of Europe, driving the surface concentrations of pollutants down without any change in emissions compared to the 'business as usual' (BAU) situation.

At the end of March 2020, CAMS opened a web page (<https://bit.ly/3jVym4W>) to gather relevant information from its portfolio of products and make results more readily accessible. The idea was to respond to the high demand from epidemiologists, media and the general public (Vincent-Henri Peuch et al., 2020). This has inter alia shown a very good consistency between ground-

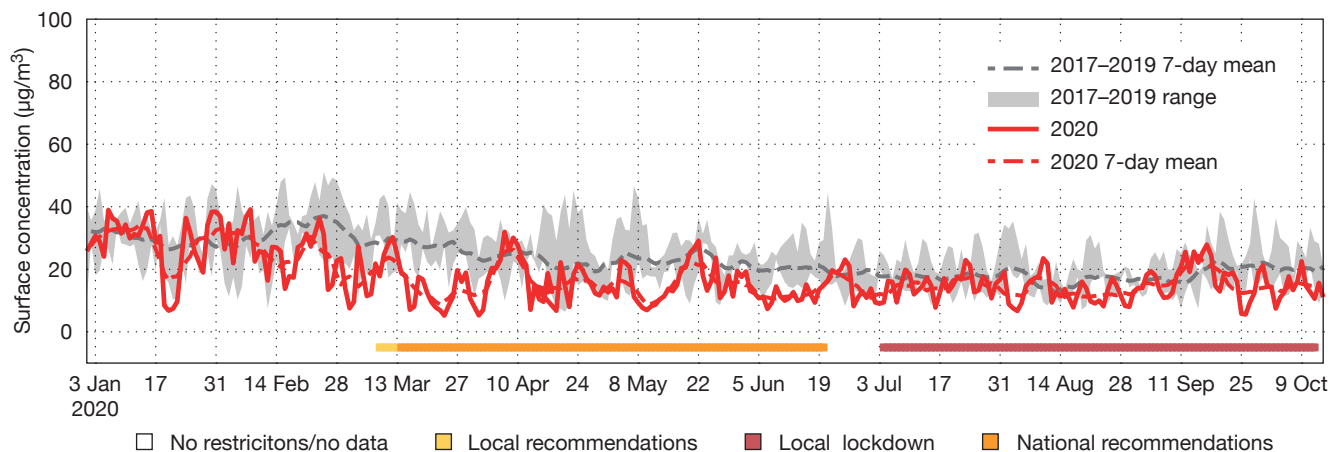


**FIGURE 1** Surface concentrations of NO<sub>2</sub> from the CAMS regional daily analyses for the city of Barcelona between 1 January 2020 and 8 July 2020 (red) compared to the range of values observed for the same dates in 2017–2019. The data source for the local/national lockdown restrictions is the Oxford COVID-19 Government Response Tracker.

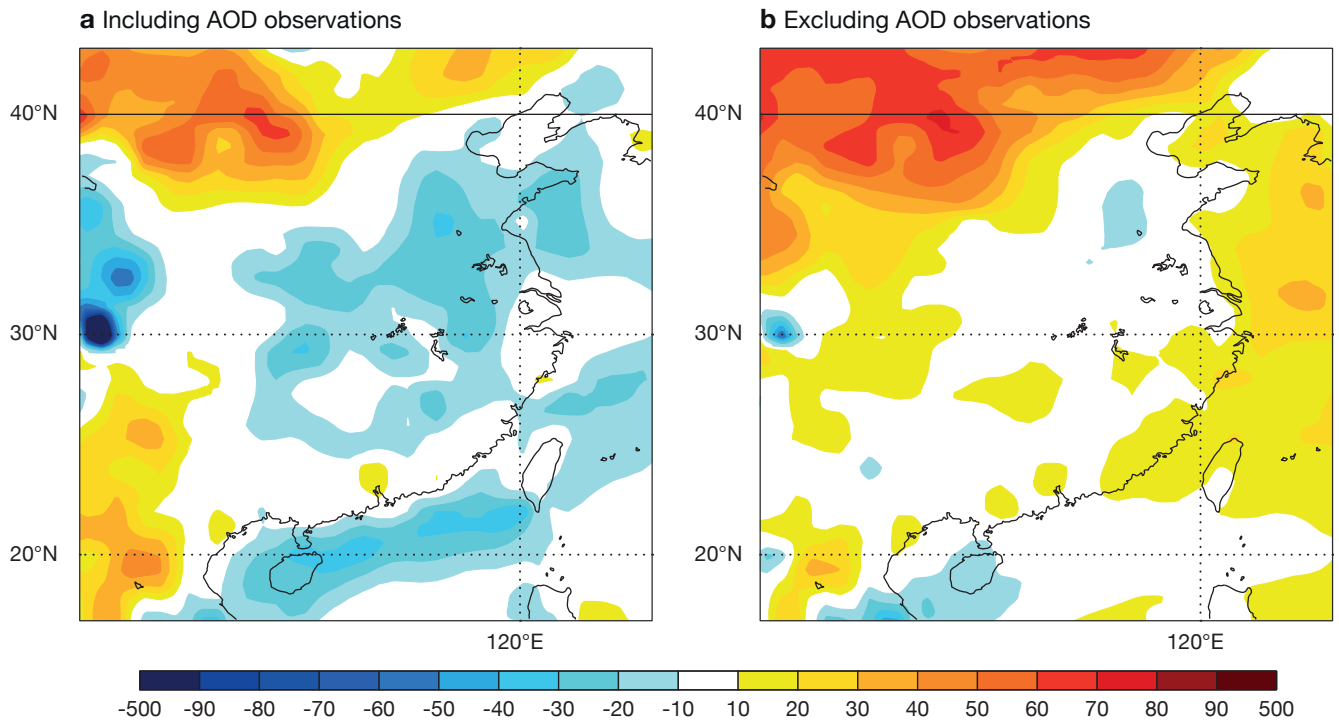


**FIGURE 2** Percentile difference of fine particulate matter (PM<sub>2.5</sub>) levels for February 2020 relative to the February mean over the years 2017–2019 as monitored by CAMS (a) including the assimilation of AOD observations and (b) excluding the assimilation of AOD observations.

based and satellite estimates of NO<sub>2</sub>, confirming that measuring air quality from space has become a reality with Sentinel-5P/TROPOMI. It also facilitated a very strong uptake of CAMS information in top tier media outlets throughout the spring season, confirming ECMWF Copernicus as a go-to source for fast and accurate information and expertise about air pollution. Importantly, CAMS helped convey caveats about the interpretation of data, pointing to the importance of considering weather aspects but also to the importance of sampling and cloud contamination in the case of satellite data (<https://bit.ly/3jVdvif>). The next two sections will show how CAMS products helped to shed light on the COVID-19 and air pollution links.

## Focus on China and Europe

The work of the CAMS team for estimating air pollution changes due to COVID-19 measures first focused on China (<https://bit.ly/3nLrp92>). Because of the lack of real-time access to surface observations, the work used satellite Aerosol Optical Depth (AOD) data from the two NASA MODIS instruments and concentrated on PM<sub>2.5</sub>. The CAMS global system, the COMPO configuration of the Integrated Forecasting System (IFS), includes estimates of emissions. It ignores the changes due to the lockdown measures in place in February 2020 and is thus representative of what would have happened under BAU conditions. As depicted in Figure 2, we have compared the February 2020 anomaly in surface PM<sub>2.5</sub> compared to the average of February 2017–19 in the analyses

assimilating AOD observations (left) and in the control run without data assimilation (right). Because of the assimilated observations, the former is capable of capturing the actual situation of February 2020 in China (including effects of lockdown) while the latter is an estimate of what would have happened if there had been no pandemic and no restriction measures. What the figure shows is that, while from an interannual point of view no marked anomaly for 2020 compared to the three previous years would have been expected under BAU conditions (right panel), PM<sub>2.5</sub> concentrations were lower by 20 to 30% over large parts of China (left panel), giving a first quantitative measure of the effect of lockdown over this region.

CAMS continued to work on this topic, focusing on Europe and refining the methodologies used to address the question of the air quality changes. Barré et al. (2020) report a very innovative method, which combines Sentinel-5P/TROPOMI data and machine learning (ML). In order to estimate the changes, an ML algorithm was trained on 2019 and used to estimate 2020 BAU values, for the purpose of comparing with the actual measurements of the satellite in 2020. This allowed changes in NO<sub>2</sub> to be estimated across all the cities in Europe with above 500k inhabitants, giving estimates ranging from about 50 to 60% for Madrid, Turin and Milan, down to less than 20% for Stockholm or Belgrade.

CAMS also worked in parallel on another approach using the ensemble of 11 regional air quality models

used for daily forecasting: CHIMERE (Ineris, France), DEHM (Aarhus University, Denmark), EMEP (Met Norway), EURAD-IM (Cologne University, Germany), GEM-AQ (WUT/IEP, Poland), LOTOS-EUROS (TNO/KNMI, the Netherlands), MATCH (SHMI, Sweden), MINNI (ENEA, Italy), MOCAGE (Météo-France), MONARCH (BSC, Spain) and SILAM (FMI, Finland). These models have been run over the period mid-March to end of April under the coordination of Ineris (France) using two sets of emissions: one corresponding to BAU conditions and the other to a COVID-19 emissions dataset for the first period of generalised lockdown between mid-March and the end of April.

The COVID-19 emissions dataset has been prepared by the Barcelona Supercomputing Centre by working with publicly available data, such as mobility/traffic information available from Google and Apple, energy statistics from the European Network of Transmission System Operators for Electricity or flight activity reports (Guevara et al., 2020). Daily emission change factors have been developed for five of the most affected activity sectors including: road transport, energy and manufacturing industry, aviation, residential & commercial and shipping. Figure 3 shows the weekly evolution of emissions of Nitrogen Oxides in Spain over the first half of 2020. It shows a sharp decrease of up to about 50%, especially marked in week 11 (March 9 to 15), followed by a slow recovery starting in week 21 (May 18 to 24). It is estimated that at the end of July, activity levels were still not up to normal (about 10% down). The sectors with stronger reductions were road transport and aviation, although the latter only represents a very small fraction of total Spanish emissions.

With these COVID-19 emissions on the one hand and the BAU ones on the other hand, the 11-member ensemble has been run and provided estimates of the changes in key pollutant concentrations. These results factor in the effect both of emissions reduction and of the specific meteorological conditions. Figure 4 depicts the relative difference between the two ensembles of runs for NO<sub>2</sub> and PM<sub>10</sub>. The map shows differences of up to about 60% for NO<sub>2</sub> and 20% only for PM<sub>10</sub>. This is because one of the most affected sectors, road transport, represents a much larger fraction of the total Nitrogen Oxides emissions than of the total Particulate Matter emissions. The maps also show marked differences across Europe regarding the reductions that are found. Nicely, the quantitative findings are fully consistent with the other approach based on Sentinel-5P and ML, although the two results are based upon entirely different methodologies. These studies have been shared with the European Environment Agency (EEA) to complement their work based on surface observations in the 'Air quality in Europe' report that the Agency publishes annually. It has to be noted

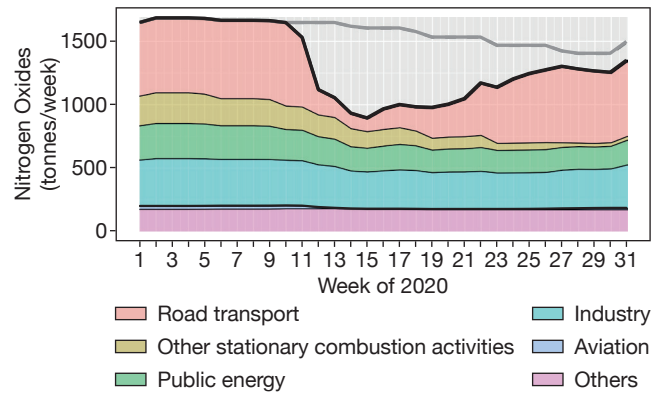


**FIGURE 3** Weekly evolution of Nitrogen Oxides emissions in Spain between week 1 and week 31 of 2020 (thick black line) compared to BAU (grey line).

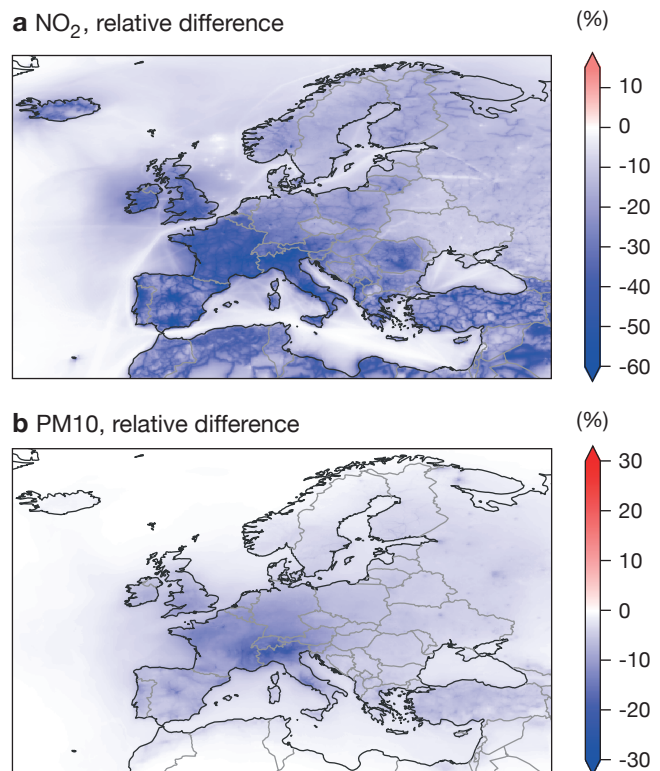


**FIGURE 4** Relative difference over 1 March 2020 to 30 April 2020 in average surface concentrations of (a) NO<sub>2</sub> and (b) PM<sub>10</sub>, calculated between two 11-member regional air quality ensembles of runs (median of the ensemble), one using 'business as usual' emissions and the other using 'COVID-19 emissions'.

that these reductions concern so-called background concentrations, which is what the CAMS regional air quality models can capture, operating at 10 km x 10 km horizontal resolution. At the local scale, for instance next to a busy road, reductions are expected to have been much larger.

## Epidemiology

Estimating such changes is an important input for epidemiologists. For instance, scientists at the London

School of Hygiene and Tropical Medicine, working in collaboration with the Multi-Country Multi-City collaborative research network, are using the inputs from the CAMS BAU vs COVID-19 model simulations. They do this by carrying out epidemiological analyses under different exposure scenarios, in order to quantify the health impacts of the air pollution changes during the period. This will be an important contribution for the a posteriori analysis of the COVID-19 pandemic, as reductions in NO<sub>2</sub> and PM10 over parts of Europe are expected to have decreased the number of deaths due to air pollution.

Of course, another more fundamental reason for looking into air quality and COVID-19 connections is that it is speculated that exposure to air pollution could be a factor in reducing the immune response and be conducive to higher infection rates. While this is fairly well-established in animals and for other diseases like seasonal influenza, it had to be assessed in the case of COVID-19. In fact, there are two slightly different questions: one is about short-term (episodic) exposure to air pollution events and the second is about long-term exposure to chronically high levels of air pollution. For such studies, CAMS data are very well suited, as analyses and reanalyses allow information to be obtained about exposure if one knows where people have been living in the years before and during 2020. CAMS has partnered with a large cohort study led by the Hopitaux de Strasbourg (France), which has obtained detailed data about over a thousand elderly people in France and Belgium. The analysis of their exposure since January 2018 and during the first months of 2020 is in progress using CAMS data about main air pollutants, UV radiation and weather parameters, in partnership with the University of Harvard (USA). Such detailed studies take time and the international literature already provides results from correlative studies, which are faster to conduct but may lead to spurious effects as correlation is not causation. Some figures have appeared, such as exposure to +1mg/m<sup>3</sup> PM2.5 for 10 years could equate to +8% in COVID-19 deaths in a study over the USA (Wu et al., 2020). Some of these studies used CAMS data for their work, such as Borro et al. (2020). They mention using CAMS because of the complete spatio-temporal coverage offered and because of its quality: “The CAMS near-real-time reanalysis is the most recent global reanalysis data set of atmospheric composition and air quality, with a demonstrated unprecedented level of accuracy and space–time resolution.” The study looked into the case of 110 Italian provinces over the period 20 February to 31 March 2020 (short-term exposure). It investigated positive correlations between PM2.5 levels and the incidence ( $r = 0.67$ ), the mortality rate ( $r = 0.65$ ) and the case fatality rate ( $r = 0.7$ ) of

COVID-19. Another area of investigation, more putative, is the potential role of aerosols (fine particulate matter in suspension in air) as vectors for the SARS-CoV-2 virus. In principle, airborne transmission of the virus can occur through inhalation of PM2.5 particles, which could stay airborne for a few hours. While the phenomenon is most probably effective indoors (with some decisive measurements made in some hospitals), current thinking is that it is a minimal route of contamination outdoors. More work is in progress about this.

## Conclusion

CAMS has made some decisive contributions to the study of possible links between COVID-19 and air quality, especially in China and Europe. It has done this by comparing expected air quality based on normal levels of activity with analysed air quality based on actual levels of activity. CAMS has also contributed to studies of the health impacts of the air pollution changes during the period and the possibility that exposure to air pollution could be a factor in reducing the immune response. Finally, CAMS has been very actively supporting the World Meteorological Organization’s Global Atmospheric Watch programme in organising international efforts looking at these different questions. Over one hundred groups from all over the world have been working on similar questions and, as results are becoming available, it will be possible to confront and consolidate the findings.

## Further reading

**Borro, M., P. Di Girolamo, G. Gentile, O. De Luca, R. Preissner, A. Marcolongo et al.**, 2020: Evidence-Based Considerations Exploring Relations between SARS-CoV-2 Pandemic and Air Pollution: Involvement of PM2.5-Mediated Up-Regulation of the Viral Receptor ACE-2, *Int. J. Environ. Res. Public Health*, **17**, 5573.

**Barré, J., H. Petetin, A. Colette, M. Guevara, V.-H. Peuch, L. Rouil et al.**, 2020: Estimating lockdown induced European NO<sub>2</sub> changes, *Atmos. Chem. Phys. Discuss.*, under review, doi:10.5194/acp-2020-995.

**Guevara, M., O. Jorba, A. Soret, H. Petetin, D. Bowdalo, K. Serradell et al.**, 2020: Time-resolved emission reductions for atmospheric chemistry modelling in Europe during the COVID-19 lockdowns, *Atmos. Chem. Phys. Discuss.*, under review, doi:10.5194/acp-2020-686.

**Peuch, V.-H., C. Buontempo & R. Engelen**, 2020: Copernicus contributes to coronavirus research, *ECMWF Newsletter No. 164*, 8–9.

**Wu, X., D. Braun, J. Schwartz, M.A. Kioumourtzoglou & F. Dominici**, 2020: Air pollution and COVID-19 mortality in the United States: Strengths and limitations of an ecological regression analysis, *Science advances*, **6**, p.eabd4049.

## Progress towards a European Weather Cloud

Florian Pappenberger, Martin Palkovič

One of ECMWF’s objectives as defined in its Convention is to make the results of the Centre’s research and operations available to its Member States “in the most appropriate form”. Today, as the volume of data produced at ECMWF continues to grow, cloud technology is becoming the only realistic way to meet this objective. A key advantage of cloud technology is that it can be used to carry out data processing where the data is, without the need to transfer or download large volumes of data. That is why, in December 2018, ECMWF’s Council approved a two-year pilot project to create, jointly with EUMETSAT, a federated cloud computing infrastructure focused on meteorological data. Dubbed the European Weather Cloud, it will mainly serve the European Meteorological Infrastructure (EMI) and its users (Box A). As the initial two-year pilot period draws to a close, substantial progress has been made in addressing the project’s governance and infrastructure aspects and in trialling use cases. The European Weather Cloud is expected to become operational in 2022 after extending the pilot phase by another year (Figure 1).

By creating a joint European Weather Cloud, ECMWF and EUMETSAT will build the foundations for a strong European IT infrastructure enabling direct access to and processing of both organisations’ data holdings. This means that observation data, forecast data and meteorological products can be accessed together as if they were collocated. Federation with other relevant cloud infrastructures in our Member States via a dedicated interface will make it possible to further widen the range of accessible data. Such a cloud infrastructure offers significant advantages and has the potential to evolve into a game changer in the way ECMWF, EUMETSAT and Member State data and products are

used in the future by their user communities.

### Motivation

ECMWF’s operational outputs are constantly growing. At the beginning of 2018, the Centre’s overall production corresponded to 90 terabytes (TB) of data per day. This is projected to rise to 360 TB by 2022 and to exceed 1 petabyte (PB) by 2026. Today, only about 35 TB of data is disseminated to users every day. The high data volume and lengthy data transfer times are likely to be part of the explanation why only a relatively small proportion of the data produced reaches users. Cloud computing and big data technologies are now sufficiently mature to allow users to make more extensive use of ECMWF products.

The basic idea is to bring users to the data instead of transferring the data to users. This is becoming even more important as the Centre moves towards higher-resolution global ensemble forecasts. Decreasing the grid spacing of such forecasts from about 18 km today to a few kilometres, in line with ECMWF’s Strategy, will greatly increase the size and complexity of the data volumes produced at the Centre. Cloud technology will enable our Member States and other users to fully exploit the benefits of such data.

In addition, a key idea behind the European Weather Cloud is to bring together data holdings from across the entire EMI in a single federated cloud infrastructure. This will make it possible to access and process multiple datasets, separately or in combination, for the mutual benefit of all entities participating in the European Weather Cloud.

### Key concepts

There are three broad layers of services that can be provided on a cloud computing infrastructure:



FIGURE 1 Anticipated timeline from the first quarter of 2020 to the operational phase of the European Weather Cloud.

- **Infrastructure as a service (IaaS):** this basic cloud computing layer provides computing, network and storage capabilities. Users can commission virtual machines or collections of containers with characteristics of their choice (operating system, number of CPUs, amount of memory, disk volumes...) that they can then start, stop or decommission according to their needs.
- **Platform as a service (PaaS):** this layer provides access to standard off-the-shelf software and services, such as databases or web servers. Users then build applications that rely on these services but would not necessarily be aware of the systems on which these processes are running.
- **Software as a service (SaaS):** this layer provides end-user-facing applications. Users interact with them using a web browser and are entirely unaware of the supporting infrastructure.

It is anticipated that all these services will be provided as part of the European Weather Cloud.

A key characteristic of the European Weather Cloud is that it will have a federation capability. This will make it possible for an entity of the EMI (e.g. an ECMWF Member State or a group of Member States) to be connected to the European Weather Cloud via the federation interface (Figure 2). The data holdings of this entity would then become discoverable and accessible for use within the rest of the European Weather Cloud. In turn, the entity's users would be able to access and use all European Weather Cloud data.

Using the federative capability of the European Weather Cloud could be of interest to large national meteorological and hydrological services (NMHS) or to groups of smaller NMHSs with a common thematic or geographic focus. The structure works with two further concepts:

- **Portal:** The federation layer is delivered through a web portal, which can orchestrate many clouds. Each member of the federation offers a different door to access the federated cloud services through a single European Weather Cloud Portal.
- **Tenants:** Each project with access to the European Weather Cloud is called a Tenant. Tenants are isolated environments with unique users and workloads, with no access or visibility to other Tenants in the same infrastructure.

## Governance

The European Weather Cloud will have a three-tier decision-making structure, which is already being applied in the pilot phase. At the top is a common decision layer for governance and management decisions taken by ECMWF and EUMETSAT with their

## a Prospective users of the European Weather Cloud

The European Weather Cloud will mainly serve the European Meteorological Infrastructure (EMI) and its users. The EMI comprises several European organisations that are active in the field of meteorology as well as the national meteorological and hydrological services (NMHSs) which they bring together. These organisations are EUMETSAT, ECMWF, EUMETNET (a network of 31 NMHSs) and ECOMET (an economic interest grouping comprising 28 NMHSs).

In addition, in June 2020 ECMWF's Council agreed that the European Weather Cloud can also be used by the NMHSs of the World Meteorological Organization and by research organisations for activities aligned with ECMWF's mission.

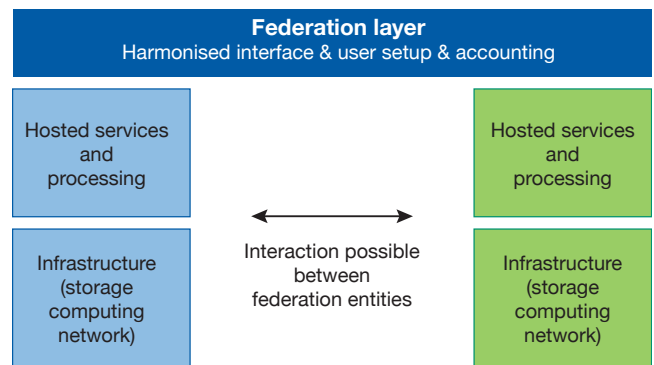


**FIGURE 2** The European Weather Cloud will be a federation of different entities held together by a federation layer. Users can interact with different entities. By interacting with one, they can also access the others. Their European Weather Cloud activities are logged centrally in the federation layer.

Councils and Committees. There follows a common coordination layer for implementation and operation activities carried out by a Technical Coordination Team. This also provides support for decisions to be taken at the governance level. A local layer is responsible for activities that need to be communicated to other entities of the federation without requiring coordination (Figure 3).

## Infrastructure

The design, procurement and deployment of hardware for the initial configuration of the infrastructure have

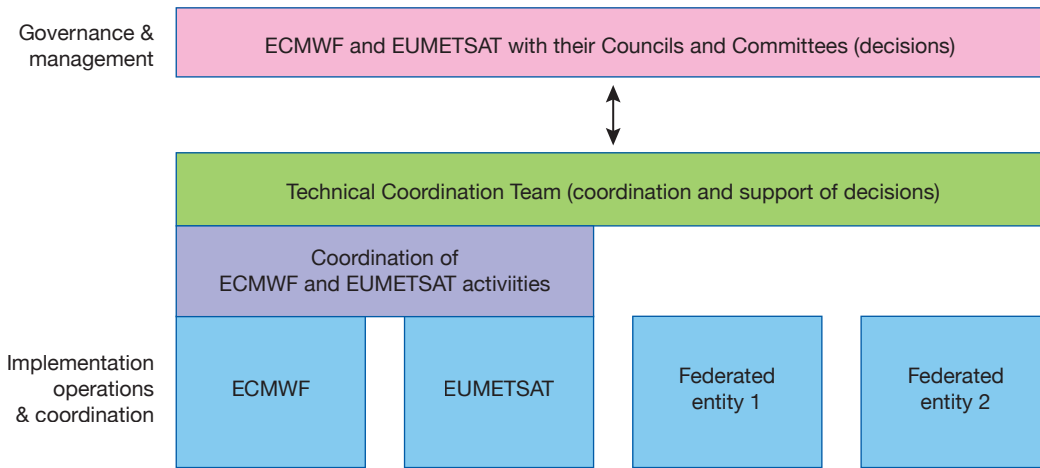


**FIGURE 3** Governance and coordination structure for the European Weather Cloud. While the Councils and Committees are in charge of the governance and direction of the cloud, the cloud entities themselves implement the necessary systems and coordination between the federated entities.

been completed. Below the federation layer, the European Weather Cloud pilot infrastructure at ECMWF comprises two components: a storage platform based on Ceph and a cloud computing platform based on OpenStack, which allow users to create on-demand virtual resources.

Evaluation reports commissioned by ECMWF for its OpenStack and Ceph clusters have found that those systems are performing well and as expected. Recent additions to the infrastructure, like GPUs, make it possible to support resource-demanding artificial intelligence and machine learning workloads. The Ceph cluster has been expanded to further improve its I/O performance.

The ECMWF component of the European Weather Cloud will be part of the Centre’s computing capacity available to Member States as outlined in the ECMWF Convention. It will also complement the other computing services available at ECMWF and will be integrated with them. It will be a resource for official Member State duties, predominantly for the purpose of processing ECMWF data and serving products to Member and Co-operating States.

## Use cases

For the pilot project, 29 use cases have been defined and are at various stages of development. In addition, an unscheduled use case arose in March this year, when an earthquake damaged the building of the Croatian Meteorological and Hydrological Service (DHMZ). Within days, DHMZ managed to back up its operational production and essential services on ECMWF’s High-Performance Computing Facility and the European Weather Cloud. More details on how this was done can be found in a previous ECMWF Newsletter article by Abellan et al. (2020). The pilot project use cases are mostly aimed at users in the developers’ own organisations. They include:

- Running web services to explore hosted datasets

- Running an atmospheric dispersion model on ECMWF forecast data
- A platform to support the training of machine learning models on archive datasets
- Research in collaboration with external partners.

For example, the German weather service DWD is already feeding maps generated by a server it deployed on the cloud into its public GeoPortal service; a joint EUMETSAT and ECMWF use case will assess bias correction schemes for the assimilation of radiance data based on several satellite data time series; the Royal Netherlands Meteorological Institute (KNMI) will host a climate explorer web application based on KNMI climate explorer data and ECMWF weather and climate reanalyses; the Royal Meteorological Institute of Belgium will prepare ECMWF forecast data for use in a local atmospheric dispersion model; and the EUMETSAT Numerical Weather Prediction Satellite Application Facility (NWP SAF) will develop a training module for a fast radiative transfer model (RTTOV) based on ERA5 reanalysis data.

A joint ECMWF–EUMETSAT user workshop took place on 27 May 2020. The online event was attended by nearly 200 participants at peak times and provided valuable feedback for developing the future cloud service. For more details, see the ECMWF Newsletter article by Siemen et al. (2020). A further virtual ECMWF–EUMETSAT workshop on the European Weather Cloud took place on 10 November 2020.

## Pilot federation

The federation capability offered by the European Weather Cloud increases data access for all parties and creates opportunities for processing schemes and applications that were previously not feasible. The underlying principle is to respect the identities of the federated entities and their responsibility for the data. The pilot phase of the European Weather Cloud

aims to gather experience in operating such a scheme, initially with a few pilot federations before opening it up to a larger number of NMHSs.

The main aspects of the federation that will be tried out and analysed during the pilot phase relate to identifying technical constraints; validating a framework of reciprocal commitments, rights and responsibilities; validating management and coordination aspects with the federated entities; and demonstrating the benefits of the scheme. The selection of entities participating in the pilot federation is based on their technical readiness and availability for making the required commitments.

## Web presence

A European Weather Cloud website has been set up at: <http://www.europeanweather.cloud>. At this stage, the main aim of the site is to enable potential users to find online information on the project's purpose and current status. In the longer term, it is expected that this website will host support pages, the catalogue of available data and services, and system status information. A European Weather Cloud Knowledge Base page has also been created at <https://confluence.ecmwf.int/display/EWCLLOUDKB> as a joint effort with EUMETSAT along with a support platform demonstrating the synergies and benefits of working together. This page provides technical details and other information and is intended for pilot users.

## Outlook

After nearly two years of the pilot phase of the European Weather Cloud, substantial progress has been made on all aspects of this major project: governance, infrastructure, use cases, federation and web presence. The usefulness of the European Weather Cloud has already been demonstrated by the role it played in backing up Croatia's forecast production following an earthquake earlier this year. Other use cases are also showing great promise by demonstrating the value of combining datasets and processing data in the cloud. The focus for the year ahead will be on further developing and evaluating the use cases. The results will feed into configuration decisions for the operational phase, which is expected to begin in 2022.

## Further reading

**Abellan, X., K. Horvath, I. Pelajić & A. Stanešić**, 2020: Croatian met service backs up its production at ECMWF after earthquake, *ECMWF Newsletter* **No. 164**, 5–7.

**Siemen, S., X. Abellan, C. Simarro, J. Saalmüller, M. Grant & J. Schulz**, 2020: User workshop aids European Weather Cloud development, *ECMWF Newsletter* **No. 164**, 16.

## Contact information

ECMWF, Shinfield Park, Reading, RG2 9AX, UK

Telephone National 0118 949 9000

Telephone International +44 118 949 9000

Fax +44 118 986 9450

ECMWF's public website [www.ecmwf.int/](http://www.ecmwf.int/)

E-mail: The e-mail address of an individual at the Centre is [firstname.lastname@ecmwf.int](mailto:firstname.lastname@ecmwf.int). For double-barrelled names use a hyphen (e.g. [j-n.name-name@ecmwf.int](mailto:j-n.name-name@ecmwf.int)).

For any query, issue or feedback, please contact ECMWF's Service Desk at [servicedesk@ecmwf.int](mailto:servicedesk@ecmwf.int).

Please specify whether your query is related to forecast products, computing and archiving services, the installation of a software package, access to ECMWF data, or any other issue. The more precise you are, the more quickly we will be able to deal with your query.

## ECMWF publications

(see [www.ecmwf.int/en/research/publications](http://www.ecmwf.int/en/research/publications))

### Technical Memoranda

- 873 **Johannsen, F., L. Magnusson & E. Dutra:** Evaluation of biases and skill of ECMWF Summer sub-seasonal forecasts in the Northern Hemisphere. *October 2020*
- 872 **Lopez, P.:** Quality Control for GOES Geostationary Lightning Mapper Level-2 flash products. *October 2020*
- 871 **Zsótér, E., H.L. Cloke, C. Prudhomme, S. Harrigan, P. de Rosnay, J. Munoz-Sabater & E. Stephens:** Trends in the GloFAS-ERA5 river discharge reanalysis. *September 2020*
- 870 **Massart, S., N. Bormann, M. Bonavita & C. Lupu:** Skin Temperature Analysis for the Assimilation of Clear-Sky Satellite Radiances. *August 2020*

- 869 **Polichtchouk, I., S. Malardel & M. Diamantakis:** Potential temperature as a prognostic variable in hydrostatic semi-implicit semi-Lagrangian IFS. *August 2020*
- 868 **Beljaars, A.:** Towards optimal parameters for the prediction of near surface temperature and dewpoint. *July 2020*

### ESA Contract Reports

**Weston, P. & P. de Rosnay:** Quality Control Plan for Brightness Temperature Modelling. *October 2020*

### EUMETSAT/ECMWF Fellowship Programme Research Reports

- 55 **Duncan, D. & N. Bormann:** On the Addition of Microwave Sounders and NWP Skill, Including Assessment of FY-3D Sounders. *September 2020*

## ECMWF Calendar 2020/21

Dec 1	Machine learning seminar series – Enhancing Western United States Sub-Seasonal Forecasts	May 17–20	Joint ECMWF/OceanPredict workshop on Advances in Ocean Data Assimilation
Dec 8–9	Council	May 17–21	Online computing training week
Feb 1–4	Training course: Use and interpretation of ECMWF products	Jun 1–4	Virtual event: Using ECMWF's Forecasts (UEF2021)
Feb 8–10	Virtual workshop: Weather and climate in the cloud	Jun 29–30	Council
Mar 15–19	Training course: Parametrization of subgrid physical processes	Jun 29 – Jul 1	Workshop on hydrological prediction and applications
Mar 22–26	Training course: Predictability and ensemble forecast systems	Sep 13–17	Virtual event: Annual Seminar 2021
Apr 12–16	Advisory Committee for Data Policy and data policy meetings of EUMETSAT and ECOMET	Sep 20–24	19th Workshop on High-performance Computing in Meteorology
Apr 27–28	Finance Committee	Sep 27–30	Radio-Frequency Interference Workshop
Apr 28	Policy Advisory Committee	Oct 4–7	Training course: Use and interpretation of ECMWF products
May 4–7	Training course: Advanced numerical methods for Earth system modelling	Oct 4–6	Scientific Advisory Committee
May 10–14	Training course: Data assimilation	Oct 7–8	Technical Advisory Committee
		Oct 27–28	Finance Committee
		Oct 28	Policy Advisory Committee
		Dec 2–3	Council



**Newsletter** | **No. 165** | Autumn 2020

European Centre for Medium-Range Weather Forecasts

[www.ecmwf.int](http://www.ecmwf.int)